

## **REMARKS**

In the Office Action dated November 2, 2006, claims 1-40 are pending, of which claims 2, 4, 6, 10-17, 21 and 24-39 are withdrawn from further consideration as directed to non-elected subject matter. Claims 1, 3, 5, 7-9, 18-20, 22-23 and 40 are examined and are rejected. Specifically, Claims 18 and 23 are rejected under 35 U.S.C. §112, second paragraph, as indefinite. Claims 18, 20 and 23 are rejected under 35 U.S.C. §112, first paragraph, for lacking complete deposit information. Claims 1, 3, 5, 7-9, 18 and 22-23 are rejected under 35 U.S.C. §112, first paragraph, as allegedly failing to satisfy the enablement requirement. Claims 1, 3, 18 and 23 are separately rejected under 35 U.S.C. §112, first paragraph, for lacking enablement. Claims 1, 3, 5, 7-9, 18-20, 22-23 and 40 are rejected under 35 U.S.C. §102(e) as allegedly anticipated by PamI et al. (U.S. Published Application 2003/0092009). Additionally, the Examiner requires Applicants to submit a certified copy of the parent application, PCT/AU02/01246.

This Response addresses each of the Examiner's objections and rejections. Applicants therefore respectfully submit that the present application is in condition for allowance. Favorable consideration of all pending claims is therefore respectfully requested.

Initially, Applicants requested in the previous Response, filed July 31, 2006, that the Examiner also include claim 6 in the examination, as claim 6 depends on claim 5 and recites the most preferred types of cancers in the context of performing the instant diagnostic method. The Examiner has not addressed Applicants' request in the pending Office Action. Applicants respectfully submit that at the very least, claim 6 should be rejoined in the examination if the generic claims are found allowable.

With respect to Applicants' priority claim, the Examiner has acknowledged Applicants' submission of a certified copy of Australian Provisional Application PR7618/01. However, the Examiner contends that this priority document does not provide support for a method of detection involving an antibody to LM04 secreted by hybridoma 16H2 or 20F8. Furthermore, the Examiner requires Applicants to submit a certified copy of the parent application, PCT/AU02/01246.

It is understood that the Examiner's determination of Applicant's priority is directed to the use of an antibody to LM04 specifically secreted by hybridoma 16H2 or 20F8. Applicants respectfully submit that the priority document PR7618/01 provides an extremely extensive disclosure of the generation and use of antibodies that are specific for LM04, notwithstanding the fact that the document may not specifically disclose the monoclonal antibody 16H2 or 20F8.

Furthermore, Applicants are providing herewith a certified copy of PCT/AU02/01246. As such, Applicants' priority claim with respect to PCT/AU02/01246 is perfected.

Claims 18 and 23 are rejected under 35 U.S.C. §112, second paragraph, as indefinite for reciting the terms "derived from" and "derived part". Even though the Examiner agrees with Applicants that these terms are commonly used, the Examiner maintains that the metes and bounds of the claims cannot be determined. The Examiner previously requested Applicants to clarify whether the terms "derived from" and "derived part" mean "obtained from" and "obtained part", respectively.

In an effort to favorably advance prosecution of the present application, Applicants have amended claims 18 and 23 to replace the terms "derived from" and "derived part" with "obtained from" and "obtained part", respectively. It is respectfully submitted that the claims, as

presently amended, are not indefinite. Withdrawal of the rejection under 35 U.S.C. §112, second paragraph, is respectfully requested.

Claims 18, 20 and 23 are rejected under 35 U.S.C. §112, first paragraph, for lacking complete deposit information.

Applicants respectfully submit that copies of the deposit receipts for hybridoma cell lines 16H2 and 20F8 were provided in the Response filed on August 4, 2006. As indicated in the receipts, the deposits were made in accordance with the provisions of the Budapest Treaty. In that Response, the undersigned, as Applicants' attorney, also made the statement with respect to the availability of the deposited materials, as required.

During a telephone interview conducted on January 17, 2007, the undersigned sought clarification from the Examiner as to the basis of the rejection. Apparently the Examiner had believed, erroneously, that the statement respecting availability need to be provided by the applicant or the assignee in an affidavit or declaration. The Examiner agreed with the undersigned during the interview that a statement made by an attorney of record should be sufficient and the rejection would be withdrawn. Accordingly, the rejection under 35 U.S.C. §112, first paragraph, with respect to the deposits, is obviated.

Claims 1, 3, 5, 7-9, 18 and 22-23 are rejected under 35 U.S.C. §112, first paragraph, as allegedly failing to satisfy the enablement requirement.

The Examiner indicates that claim 23 still recites "derivatives", "mutant" and "variant", even though it was stated in the previous Response that such terms were deleted from the claims.

By way of the instant amendment, Applicants have amended claim 23 to delete these terms objected to by the Examiner.

Furthermore, the Examiner maintains that the specification does not disclose any functional or structural attributes of an immunointeractive molecule other than antibodies, or any immunointeractive molecule other than an antibody that is immunoreactive to LM04 and forms a complex with LM04. Applicants previously submitted that the specification discloses other immunointeractive molecules, such as antibody fragments, single chain antibodies, deimmunized antibodies and T-cell associated antigen-binding molecules (TABMs). In response, the Examiner states in the pending Action that the term "immunointeractive molecule", as defined in the specification, encompasses any (i.e., all) compounds, including small molecules, proteins, or even nucleotides, as long as such molecule binds to LM04 and forms a complex with LM04.

Applicants respectfully disagree with the Examiner's position that reference to the term "immunointeractive molecule" would extend to all compounds such as any small molecule or nucleotide. In the first instance, the fact that the molecule is classified as "immunointeractive" indicates that the molecule interacts via an immunological mechanism and not merely by any binding mechanism which would apply to any small molecule or other compound. The generally recognized immunological mechanisms are those which attach to antibody and T-cell receptor like interactions and which therefore require antibody-like or T-cell receptor-like molecules.

Applicants further respectfully submit that it is a well known concept that antibody specificity for diagnostic or therapeutic purposes extends well beyond conventional monoclonal antibody structure to, for instance, divalent, trivalent and single chain forms that retain target specificity. That specificity, however, is rendered possible by virtue of the immunological nature of the binding interaction that occurs. This is a distinct form of specificity, which does not compare and bears no similarity to the specificities which other small molecules may show in terms of their function. To support Applicant's position, the following citations are provided:

Hollinger et al. (1999) (abstract attached as **Exhibit 1**), Bernd et al. (2004) (abstract attached as **Exhibit 2**), Kortt et al. (2001) (abstract attached as **Exhibit 3**), Beckman et al. (2006) (**Exhibit 4**) and Anderson et al. (2004) (**Exhibit 5**). These articles also describe the various approaches to the generation of such antibody fragments that are well known in the art.

Applicants respectfully submit that the present invention is principally based on the recognition of the relationship between LM04 and neoplastic cell development, and is not directed to the specific nature of the molecule which is used to monitor the change in the level of LM04. Therefore, Applicants respectfully submit that the claims should not be limited to certain specific molecules, which are provided in the specification as examples of immunointeractive molecules.

In view of the foregoing, Applicants respectfully submit the specification provides sufficient support for those skilled in the art to practice the invention as presently claimed, without undue experimentation. Accordingly, the enablement rejection of claims 1, 3, 5, 7-9, 18 and 22-23 under 35 U.S.C. §112, first paragraph, is overcome, and withdrawal thereof is respectfully requested.

Claims 1, 3, 18 and 23 are further rejected under 35 U.S.C. §112, first paragraph, for lacking enablement on the ground that the claimed methods employ a deimmunized antibody wherein at least one of the CDRs of the variable domain of the antibody is derived from a monoclonal antibody to LM04.

It is understood that the Examiner agrees with Applicants in that the functional limitation of forming an antibody-LM04 complex, recited in the claims, would inherently require that sufficient CDRs are derived from the anti-LM04 antibody to confer epitopic specificity. However, the Examiner argues in essence, that the specification does not provide any guidance

for making or using a deimmunized antibody having only one of the CDRs from an anti-LM04 antibody, or having a small change in the CDRs of an anti-LM04 antibody, wherein the deimmunized antibody still forms a complex with LM04.

Applicants respectfully submit that the full complement of CDRs is not required to produce a protein with the requisite antigen binding function. It has been shown in the art that single domain antibodies exhibit good antigen binding affinities, as detailed, for example, in Ward (1998) (abstract attached hereto as **Exhibit 6**) and Desmyter et al. (2001) (**Exhibit 7**). It has further been demonstrated that antibodies may be altered by replacing CDRs of an immunoglobulin with CDRs from an immunoglobulin of different specificity without any significant loss of antigen binding capacity. See, for example, U.S. Patent 5,225,539 (**Exhibit 8**), U.S. Patent 6,982,321 (**Exhibit 9**), U.S. Patent 6,808,901 (**Exhibit 10**) and Jones et al. (1986) (abstract attached hereto as **Exhibit 11**).

Accordingly, Applicants respectfully submit the present application provides sufficient guidance for one skilled in the art to practice, without undue experimentation, the claimed methods of using a deimmunized antibody containing at least one CDR derived from an anti-LMO4 monoclonal antibody. As such, Applicants respectfully submit that the enablement rejection of Claims 1, 3, 18 and 23 under 35 U.S.C. §112, first paragraph, is overcome and withdrawal thereof is respectfully requested.

Claims 1, 3, 5, 7-9, 18-20, 22-23 and 40 are rejected under 35 U.S.C. §102(e) as allegedly anticipated by Paml et al. (U.S. Published Application 2003/0092009).

According to the Examiner, Paml et al. disclose a method of detecting LM04 using an autoantibody against LM04 from serum of cancer patients. Paml et al. allegedly disclose that an antibody to LM04 and a fragment of LM04 formed a complex (Table 4), and that a disease

characterized by an abnormal growth neoplastic cells can be detected by the presence of an antibody to LM04 in patient's blood (page 18, example 2).

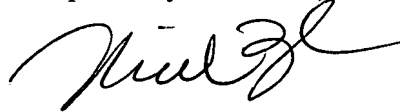
Applicants respectfully submit that the Examiner's reliance on Paml et al. is misplaced. Paml et al. describes a large list of molecular markers of cancer, which include LM04. However, with respect to the use of LM04 as a potential cancer marker, the disclosure of Paml et al. is solely directed to detection of autoantibodies against LM04. The reference does not teach anywhere that the level of LM04 *per se* in a biological sample is in any way correlated with a disease.

In particular, regarding the teaching of Paml et al. specifically relied upon by the Examiner, it is observed that Table 4 of Paml et al. lists an LM04 peptide as a potential peptide to identify tumor-specific or tumor enriched antibodies in a patient blood. See also paragraph [0061]. Page 18, example 2 of Paml et al., also referenced by the Examiner, describes the detection of autoantibodies to LM04, in contrast to the present methods which are directed to detection of LM04 (i.e., the antigen). Applicants respectfully submit that the level of autoantibodies in a sample does not necessarily reflect the level of the LM04 antigen. Changes in the expression level of a self antigen is entirely independent of the generation of auto-antibodies. In fact, by definition, since an antigen such as LM04 is a self antigen, it should normally not generate an immune response. Those skilled in the art would acknowledge that the generation of an autoimmune condition is in no way necessarily linked to an increased level of expression of a particular self antigen. Rather, the mechanisms which lead to aberrant induction of an antibody response to a self antigen are significantly more complex and generally relate to genetic factors, breakdown of tolerance mechanisms and the like.

Certainly the recognition of a correlation between the level of the LM04 antigen with a disease condition, which is provided by the present invention, is not disclosed by Paml et al., and is distinct from the observation of Paml et al. that the level of antuantibodies to LM04 can be correlated with a disease. Accordingly, the rejection under 35 U.S.C. §102(e) based on Paml et al. is overcome, and withdrawal thereof is respectfully requested.

In view of the foregoing amendments and remarks, it is firmly believed that the subject application is in condition for allowance, which action is earnestly solicited.

Respectfully submitted,



Xiaochun Zhu

Registration No. 56,311

Scully, Scott, Murphy & Presser, P. C.  
400 Garden City Plaza-STE 300  
Garden City, New York 11530  
Telephone: (516) 742-4343  
XZ:ab

Enc.:

- Certified copy of PCT/AU02/01246;
- Exhibits 1-11.



Cancer Metastasis Rev. 1999;18(4):411-9.  
Engineering antibodies for the clinic.  
Holliger P, Bohlen H.

In the last ten years recombinant 'protein drugs' such as erythropoietin or tissue plasminogen activator have become widely used in the clinic. After some early setbacks antibodies look well placed to join them. A decade of antibody engineering is finally beginning to pay off with a string of chimeric and humanized antibodies gaining the Food and Drug Administration approval in the last two years. Here we will report on recent developments in the clinical application of antibodies, in particular, in the treatment of malignant lymphoma. We will also discuss some of the current strategies for the engineering of both whole antibodies (IgG) and recombinant antibody fragments for the next generation of antibody therapeutics.

## Therapeutic Antibodies

Current Molecular Medicine, Volume 4, Number 5, August 2004, pp.539-547(9)

Bernd Groner; Cord Hartmann; Winfried Wels

Monoclonal antibodies had the lure of drugs very much since their first description. The ability to bind to a predetermined chemical structure stimulated the imagination of drug discoverers and developers. Nevertheless it took many years before a drug was registered which started to make good on the promise. The complexity of the molecule, made up of four polypeptide chains, its large molecular weight, its multiple and versatile functional domains and its mouse origin initially were obstacles for the production and the utilisation. Also the selection of appropriate target structures on the surface of cells turned out to be difficult. Many of these difficulties have been overcome. The replacement of most of the murine sequences with equivalent human sequences and the concomitant decrease in immunogenicity, and the identification of cell surface components which are causative and limiting in cellular transformation have made monoclonal antibodies valuable weapons in the fight against cancer. Multiple mechanisms of monoclonal antibody action are being exploited for this purpose. Antibodies can sequester growth factors and prevent the activation of crucial growth factor receptors. A monoclonal antibody directed against the vascular endothelial growth factor (VEGF) has been shown to be a potent neo-vascularisation inhibitor (bevacizumab). An antibody against the extracellular domain of the EGF receptor prevents the binding of the ligand to the receptor and thereby its activation (cetuximab). EGFR activity, however, is absolutely required for the survival and proliferation of certain human tumour cells. An antibody which interferes with the dimerisation of the ErbB2 and the ErbB3 members of the EGF receptor family prevents the association of a most potent signaling module (pertuxumab). The signals emanating from this dimer determine many phenotypic properties of e.g. human breast cancer cells. A monoclonal antibody also directed against ErbB2 has been most successful, clinically and commercially (trastuzumab). This antibody interferes with signals generated by the receptor and causes the arrest of the cell cycle in tumour cells. In addition, it recruits immune effector cells as cytotoxic agents. Finally, monoclonal antibody derivatives, single chain Fv fragments, have been used as a basis for the construction of recombinant tumour toxins. These molecules harness the exquisite binding specificity of the antibodies and combine them with the toxic principles of bacteria.

Biomol Eng. 2001 Oct 15;18(3):95-108. Links

Dimeric and trimeric antibodies: high avidity scFvs for cancer targeting.

Kortt AA, Dolezal O, Power BE, Hudson PJ.

Recombinant antibody fragments can be engineered to assemble into stable multimeric oligomers of high binding avidity and specificity to a wide range of target antigens and haptens. This review describes the design and expression of diabodies (dimers), triabodies (trimers) and tetrabodies (tetramers). In particular we discuss the role of linker length between V-domains and the orientation of the V-domains to direct the formation of either diabodies (60 kDa), triabodies (90 kDa) or tetrabodies (120 kDa), and how the size, flexibility and valency of each molecule is suited to different applications for in vivo imaging and therapy. Single chain Fv antibody fragments joined by polypeptide linkers of at least 12 residues irrespective of V-domains orientation predominantly form monomers with varying amounts of dimer and higher molecular mass oligomers in equilibrium. A scFv molecule with a linker of 3-12 residues cannot fold into a functional Fv domain and instead associates with a second scFv molecule to form a bivalent dimer (diabody, approximately 60 kDa). Reducing the linker length below three residues can force scFv association into trimers (triabodies, approximately 90 kDa) or tetramers (approximately 120 kDa) depending on linker length, composition and V-domain orientation. A particular advantage for tumour targeting is that molecules of 60-100 kDa have increased tumour penetration and fast clearance rates compared with the parent Ig (150 kDa). We highlight a number of cancer-targeting scFv diabodies that have undergone successful pre-clinical trials for in vivo stability and efficacy. We also briefly review the design of multi-specific Fv modules suited to cross-link two or more different target antigens. Bi-specific diabodies formed by association of different scFv molecules have been designed as cross-linking reagents for T-cell recruitment into tumours (immunotherapy), viral retargeting (gene therapy) and as red blood cell agglutination reagents (immunodiagnostics). The more challenging trispecific multimers (triabodies) remain to be described.

# Antibody Constructs in Cancer Therapy

## *Protein Engineering Strategies to Improve Exposure in Solid Tumors*

Robert A. Beckman, MD<sup>1</sup>

Louis M. Weiner, MD<sup>3</sup>

Hugh M. Davis, PhD<sup>2</sup>

<sup>1</sup> Clinical Hematology-Oncology, Centocor Research and Development, Inc., Malvern, Pennsylvania.

<sup>2</sup> Clinical Pharmacology & Experimental Medicine, Centocor Research and Development, Inc., Malvern, Pennsylvania.

<sup>3</sup> Department of Medical Oncology, Fox Chase Cancer Center, Philadelphia, Pennsylvania.

Robert A. Beckman is a full time employee of Centocor, Inc., and a stockholder in Johnson & Johnson. Hugh M. Davis is a stockholder and an employee of Centocor, Inc., a division of Johnson & Johnson.

Address for reprints: Robert A. Beckman, Clinical Hematology-Oncology, Centocor Research and Development, Inc., 200 Great Valley Parkway, Malvern, PA 19355; Fax: (610) 651-6140; E-mail: eniac1@snip.net

Received September 1, 2006; revision received October 10, 2006; accepted October 17, 2006.

© 2006 American Cancer Society  
DOI 10.1002/cncr.22402

Published online 11 December 2006 in Wiley InterScience (www.interscience.wiley.com).

Whereas over 85% of human cancers are solid tumors, of the 8 monoclonal antibodies (mAbs) currently approved for cancer therapy, 25% are directed at solid tumor surface antigens (Ag). This shortfall may be due to barriers to achieving adequate exposure in solid tumors. Advancements in tumor biology, protein engineering, and theoretical modeling of macromolecular transport are currently enabling identification of critical physical properties for antitumor Abs. It is now possible to structurally modify Abs or even replace full Abs with a plethora of Ab constructs. These constructs include Fab and Fab<sub>2</sub> fragments, scFvs, multivalent scFvs (e.g., diabodies and triabodies), minibodies (e.g., scFv-CH3 dimers), bispecific Abs, and camel variable functional heavy chain domains. The purpose of the article is to provide investigators with a conceptual framework for exploiting the recent scientific advancements. The focus is on 2 properties that govern tumor exposure: 1) physical properties that enable penetration of and retention by tumors, and 2) favorable plasma pharmacokinetics. It is demonstrated that manipulating molecular size, charge, valence, and binding affinity can optimize these properties. These manipulations hold the key to promoting tumor exposure and to ultimately creating successful Ab therapies for solid tumors. *Cancer* 2007;109:170-9. © 2006 American Cancer Society.

**KEYWORDS:** antibody, tumor exposure.

Over 85% of human cancers are solid tumors, yet of the 8 mAbs approved as cancer therapeutics as of 2005, 5 are specific to hematologic malignancies; only 3 (trastuzumab, cetuximab, and bevacizumab) can be used for solid tumors and 1 of these, bevacizumab, is directed at a soluble ligand, not at a surface protein within solid tumors.<sup>1</sup> This disproportionality reflects the challenges of achieving effective concentrations within solid tumor masses. With hematologic cancers, Abs can be readily dose-adjusted to reach the desired serum concentration. However, with solid tumors Abs are in relatively remote equilibrium with their target sites. Anatomical and physiological properties of solid tumors make them particularly hard to penetrate. Experimental data using radiolabeled Abs suggests tumor penetration is generally on the order of 0.01% of the injected dose per gram of tumor,<sup>2</sup> corresponding to a maximal intratumoral Ab concentration of approximately 100 nM, in agreement with that seen in human xenografts in mice.<sup>3-5</sup>

Recent advancements in protein engineering are bringing drug developers nearer to overcoming the barriers to developing Abs against solid tumors. Researchers can now create customized Ab-based molecules with optimized molecular size, valence, charge, and affinity.

The primary building blocks of Ab-based molecules are Fab fragments (55 kDa) and single-chain Fv (scFv; 25 kDa),<sup>6,7</sup> both of

which can be used alone or as units of larger protein constructs. Fab fragments, obtained by proteolytic digestion of IgG, include a single Ab light chain linked by a disulfide bond to a heavy chain fragment consisting of the variable region and the first heavy chain constant region, and form a single Ag binding site from the noncovalent association of heavy chain and light chain variable regions. (Fab)<sub>2</sub> fragments retain the heavy chain hinge region and are bivalent. Single-chain Fv (scFv) are single polypeptide chains incorporating a heavy chain variable and a light chain variable region, with a polypeptide linker. The heavy and light chain regions from the same chain form a single Ab-binding site. scFv molecules can also be engineered to incorporate a carboxy terminal cysteine residue, thereby enabling formation of a (scFv)<sub>2</sub> fragment by virtue of disulfide bridging.<sup>6,7</sup> Another bivalent molecule is a "diabody," which is formed from 2 scFvs linked noncovalently. Each of 2 Ag-binding sites is formed from the heavy chain variable region of 1 chain and the light chain variable region of the other, with extensive noncovalent interaction.

Diabodies have rigid, compact structures, resulting in a separation of the 2 binding sites by 65 Å, less than half the separation of the Ag binding sites within an IgG. As such, they may be ideal for bridging between cells.<sup>8</sup> A further possibility is a "minibody," in which 2 scFv fragments are linked by a component of the heavy-chain region (for example, CH<sub>3</sub>), resulting in a bivalent molecule.<sup>9</sup>

Antibodies attack tumors by 3 general mechanisms<sup>1,10</sup>: 1) opsonization, which triggers killing by immune cells, 2) modification of innate biological processes such as growth and apoptosis, and 3) delivery of a cytotoxic payload such as a chemotherapy drug, catalytic toxin, radioisotope, or enzyme. Regardless of the mechanism, unless the Ab is directed at soluble factors in the bloodstream or at tumor vascular endothelium, is conjugated to a radioisotope with a long path length, or works primarily in conjunction with immune effector cells at the periphery of the tumor, a necessary first step is penetration of the Ab into tumor tissue and binding to the target. In many cases optimal antigrowth effects are not achieved if binding is restricted to the periphery of the tumor.<sup>14</sup> Rather, the Ab must gain access to all viable cells within tumors at sufficient concentrations to effect a maximal change in the tumor.

The objective of this article is to provide a conceptual framework for capitalizing on recent scientific advancements that can promote tumor exposure. The focus is on 2 particular properties: 1) physical properties that enable penetration of and retention by tumors, and 2) favorable plasma pharmacokinetics.

## Physical Properties Governing Tumor Penetration and Retention

### *Biological properties of solid tumors*

Several barriers to transport exist within solid tumors. Solid tumors differ from normal tissue with regard to vasculature, interstitial fluid pressure, cell density, tissue structure and composition, and extracellular matrix (ECM) components.<sup>12</sup> Compared with normal tissue ECM, tumor ECM is richer in collagen, the primary determinant of tissue resistance to macromolecular transport, and is stiffer.<sup>13</sup> Measurements within murine solid tumors showed that macromolecular diffusion slowed 2-fold within 200 µm of the surface of the tumor, and more than 10-fold beyond 500 µm, correlating with increasing density of ECM and tighter collagen organization near the core of the tumor.<sup>14</sup> ECM composition differs among tumor types<sup>13,15</sup> and can also change in response to radiation therapy.<sup>16</sup>

Tumor vasculature differs from that of normal tissues in that tumor blood vessels generally are more heterogeneous in distribution, more tortuous, larger in size, and more permeable.<sup>17,18</sup> Tumor blood supplies have high viscosity, due to cells and large molecules drained from the interstitium,<sup>12</sup> resulting, together with vessel tortuosity, in greater blood flow resistance and lower blood flow relative to normal tissues.<sup>19</sup>

Vascularity is an important determinant of tumor biodistribution of Abs. In order to uniformly penetrate a tumor, an Ab or fragment must penetrate half the distance to the nearest vessel. Average intervessel distances range from 40 to 100 microns.<sup>20,21</sup> However, in areas of anatomic hypoperfusion individual intervessel distances can range up to as high as 1 mm to 1 cm.<sup>22</sup> In addition, areas of functional hypoperfusion can exist due to local elevations in interstitial pressure.<sup>23</sup> Because diffusion distance is proportional only to the square root of time, diffusion of an IgG across half a centimeter into such a region of hypoperfusion could take weeks to months. Diffusion of a smaller fragment such as scFv into this space could be 2–6-fold faster but could still take up to a month. The therapeutic relevance of penetrating these extremely hypoperfused areas depends on whether they contain viable tumor cells despite the hypoperfusion.

In solid tumors, large particles such as tumor cells commonly enter lymphatic capillaries, impairing lymphatic drainage<sup>12</sup> and decreasing the clearance of high molecular weight compounds from the tumor interstitium. This decrease in clearance, coupled with leakiness of the microvasculature, results in a tendency for macromolecules greater than 45 kDa

to be retained in solid tumors, a phenomenon termed "enhanced permeability and retention" (EPR).<sup>34</sup>

Retention of macromolecules elevates oncotic pressure, in turn drawing water into the tumor interstitium<sup>25</sup> and raising interstitial pressure compared with normal tissues. Interstitial fluid pressure is elevated uniformly throughout a tumor and drops precipitously to normal values in the tumor's periphery or in the immediately surrounding tissue.<sup>26</sup> Elevated interstitial pressure correlates with increased tumor size, decreased oxygenation, and decreased radiosensitivity.<sup>27-28</sup> Macromolecules must diffuse against this pressure gradient to penetrate tumors.

Because tumor size affects both the distance, which Abs and their fragments must diffuse to uniformly penetrate, as well as the interstitial pressure, which sets up convection currents unfavorable to penetration, larger tumor masses may be more difficult to treat with monoclonal Ab therapies. A study in colorectal patients with tumors of varying sizes, utilizing radiolabeled anti-CEA Mab, showed that the tumor penetration in percent injected dose per gram of tumor was proportional to the reciprocal of the tumor mass to the 0.362 power—i.e., approximately inversely proportional to the tumor diameter.<sup>30</sup>

#### Physical Properties of Ab Constructs That Favor Tumor Exposure

Subsequent to extravascularization, an anticancer agent must reach its binding sites on tumor cells. The agent would then ideally fully penetrate the tumor to maximize potential therapeutic efficacy. A strong molecular attraction tends to compete with tumor penetration because the agent can get stuck at the periphery. Moreover, the ability to rapidly penetrate deep into a tumor mass is often associated with suboptimal retention within the tumor. In designing antitumor constructs, a suitable balance must be found between properties that promote tumor penetration and those that promote tumor retention.

The transport of macromolecules in normal tissues is frequently by convection,<sup>25</sup> which is governed by hydraulic conductivity and pressure differences. However, within tumors, elevated and uniform interstitial pressure limits convection, and diffusion plays a prominent role in transport.<sup>15</sup> To achieve favorable tumor exposure, it is important to optimize diffusion.

A major determinant of speed of diffusion through tumors is molecular size.<sup>15,20,22</sup> The rate of diffusion is inversely proportional to the molecular radius, or approximately to the cube root of molecular weight.<sup>20,21</sup> scFv fragments diffuse approximately 6 times faster than IgG, due to their smaller size and other factors.<sup>31</sup>

Molecular charge and shape also affect tumor distribution. Because of its elongated shape and charge characteristics, IgG diffuses more slowly than dextrans of a similar molecular weight<sup>22</sup> and, indeed, the interstitial volume accessible for diffusion of an IgG is approximately one-third that of an scFv.<sup>32</sup> An analysis of 13 derivatives of scFv showed that the molecules with isoelectric points between 5 and 9 had superior tumor penetration relative to those outside this range.<sup>33</sup> These results led to the hypothesis that therapeutic proteins with isoelectric points below 5 or above 9 are prone to immobilization by electrostatic interactions with the vascular endothelium and/or extracellular matrix.<sup>33</sup>

Affinity for the target antigen (Ag) is an important variable affecting tumor distribution. Whereas one might presume that tighter binding is better, modeling by Weinstein and van Osdol<sup>34</sup> showed that tighter binding tends to result in increased retention of Ab at the periphery of 0.3-mm tumor nodules. The term "binding site barrier" was coined to describe the phenomenon of high-affinity Abs getting stuck at the tumor periphery.<sup>35</sup>

Originally, the idea that Ab affinity could increase beyond an optimum seemed counterintuitive, but it was subsequently confirmed experimentally by Adams et al.,<sup>4,5</sup> who prepared a series of radiolabeled mutant scFvs that bound to an identical HER2/*neu* epitope, but with varying affinity from  $10^{-7}$  to  $10^{-11}$  M, and studied their biodistributions in SCID mice bearing 1 mm human ovarian tumor xenografts. Biodistribution into the tumor, plasma, and normal tissues was evaluated and immunohistochemistry assessed uniformity of tumor penetration. The studies were done both in normal mice and in mice rendered anephric for 48 hours to prolong the serum half-life of the scFv.

Peak tumor: normal organ ratios and maximum tumor retentions of label were obtained with the  $10^{-9}$  M kD affinity variant. Lower dissociation constants ( $10^{-10}$  to  $10^{-11}$  M) resulted in equal tumor accumulation but less selectivity for targeting tumors. The most uniform intratumoral distribution was achieved with the scFv possessing the highest dissociation constant,  $10^{-7}$  M. Intratumoral distribution became more uniform with more time for equilibration by rendering the mouse anephric for 24 hours compared with the normal scFv half-life in mice of 3.5 hours. Thus, homogeneity of tumor penetration was optimal at a lower affinity than the affinity associated with the best tumor retention and selectivity.<sup>4</sup> In interpreting these results, one must bear in mind that radioiodinated antibodies can suffer hydrolysis of the label upon cellular internalization,<sup>36</sup> which may occur to a greater extent with a higher-affinity antibody.

To address the question of optimal affinity, Craff and Wittrup<sup>31</sup> modeled successive penetration of layers of 100- $\mu$ m tumor spheroids in the setting of Ab excess. Using parameters derived from the literature their simulations were in qualitative and quantitative agreement with a variety of experimental datasets including kinetics and dose dependence of Ab uptake into spheroids<sup>37-42</sup> and biodistribution of Abs and Ab fragments into tumor xenografts as a function of affinity, molecular weight, and elimination half-life.<sup>4,43-45</sup>

During an initial loading phase, intratumoral diffusion competes with systemic clearance, and bound Ab moves toward the tumor core, whereas the concentration of free Ab at the tumor surface remains high. Low-affinity Abs penetrate more deeply into the tumor than high-affinity Abs. Penetration of the spheroids is proportional to the free diffusion rate and to the surrounding plasma area under the curve (AUC), according to the model.

In the model's second, or retention, phase, Ag internalization or shedding depletes Ag-Ab complexes, in competition with Ag-Ab dissociation. Internalization may be associated with antitumor effect, either by cellular internalization of a toxic moiety conjugated to the Ab, or by elimination of the Ag as a cellular signaling receptor. As the affinity increases, more Ag-Ab complexes will internalize. Maximal tumor retention and exposure require Ag-Ab dissociation rates equal to or less than elimination/internalization rates, so as not to compete with this process. This corresponds to a  $K_d$  of  $10^{-9}$  to  $10^{-10}$  M for a construct with a metabolic half-life of 1 day, or to a weaker  $K_d$  for more rapidly internalizing Ags.

Jain and Baxter<sup>23,46</sup> also modeled the effect of binding, concluding that higher affinity Abs have slower penetration but increased retention. They further demonstrated that in Ab excess higher affinity is better, but in Ag excess high affinity Abs can be stuck at the periphery.

Thus, the optimal binding affinity balances 2 goals: 1) sufficiently rapid diffusion to enable penetration into the core of the tumor, and 2) sufficiently long retention to enable signaling inhibition, internalization, or other events required for a pharmacodynamic effect. Overall, the optimal  $K_d$  is governed not only by characteristics of the Ab, but by the Ag and by the requirements for therapeutic efficacy as well.

Experimental results are consistent with these theoretical principles. Yokota et al.<sup>50</sup> tested the efficacy of 3 radiolabeled Abs with affinities varying from  $4 \times 10^{-10}$  to  $4 \times 10^{-11}$  M in a murine xenograft model. The tighter binding Abs were more potent and more efficacious. However, the initial tumors were small,

about 30 mm<sup>3</sup>, and given that the attached I-131 has a radiation pathlength on the order of 1-2 mm, not much penetration would have been required.

Adams et al.<sup>4</sup> demonstrated that there was an affinity optimum for scFv, and higher affinities beyond the optimum resulted in inhomogeneous tumor penetration and decreased tumor/normal tissue selectivity.

Blumenthal<sup>47</sup> investigated the effect of total Ab dose and tumor size on uniformity of biodistribution using radiolabeled IgG1 of affinities from  $10^{-8}$  to  $10^{-9}$  M in xenografts varying in size from 0.25 to 1.5 g. Total Ag measurements by immunoassay suggested an intratumoral Ag concentration of  $10^{-7}$  M and that, at a total Ab dose of 400-500  $\mu$ g, Ag and Ab were present at 1:1 stoichiometry within the tumor. Doses of up to 800  $\mu$ g were utilized, which is 7-fold higher on a molar basis than used by Adams et al.<sup>4</sup> The IgG would have a half-life of about 100 hours in mice.<sup>48</sup> The higher doses resulted in improved homogeneity of distribution in most cases, although distribution was still heterogeneous in the larger tumors using the higher-affinity Abs. This study suggests that if dosing to Ab excess can be achieved, the "binding site barrier" may be overcome, although slow diffusion is still an issue for IgG in larger tumor masses.

Verel et al.<sup>49</sup> compared tumor biodistribution and radiotherapy efficacy of a series of 5 IgG1 Abs, with  $K_d$ s ranging from  $10^{-8}$  to  $10^{-10}$  M in a xenograft model. The lower-affinity Abs demonstrated increased tumor accumulation and radiotherapy efficacy for 100 mm<sup>3</sup> tumors at the very low dose used (20  $\mu$ g), 40-fold lower than in the Blumenthal<sup>47</sup> study.

From the above experimental and theoretical studies, it is clear that the optimal affinity for an Ag-Ab complex depends on a variety of factors, including the intervessel distance over which diffusion is required, the size of the construct, the plasma AUC over single and repeat dosing, the target Ag density, the relative intratumoral stoichiometry of Ag and Ab, and the complex dissociation rate relative to rates of Ag dissociation, elimination, and/or internalization. In general, the studies with higher Ab exposure and smaller tumors demonstrate tighter affinities at the optimum than those with larger tumors or lesser total Ab exposure. Plasma concentrations from clinical doses of trastuzumab (Herceptin) are about 1  $\mu$ M, more comparable to that achieved in the Blumenthal study,<sup>47</sup> than the lower concentrations considered in the other studies by Verel,<sup>49</sup> Adams et al.,<sup>4,5</sup> or the theoretical study that raised the binding site barrier question.<sup>35</sup>

A variety of Ab constructs have been investigated as alternatives to full Abs for diagnostic and thera-

peutic applications, exploiting the importance of molecular size in tumor biodistribution, as discussed above, and additionally exploring the role of multivalent constructs. These alternatives include Fab and Fab<sub>2</sub> fragments; scFv constructs, both monovalent and multivalent (diabodies, triabodies, and tetrabodies); minibodies (i.e., scFv-CH3 dimers); bispecific Abs; and camel variable functional heavy chain domains. In general, lower molecular weight constructs penetrate more quickly into tumors but have shorter and lower overall retention. Increased valence generally increases tumor uptake and specificity.

Thus, several groups<sup>50,51</sup> demonstrated rapid tumor uptake and plasma clearance of scFvs in a murine xenograft system, as well as more homogeneous penetration of the tumor compared with larger forms. This was also true for variable domains from camel-derived heavy chains, at 15 kDa the smallest known Ag-binding fragment.<sup>52</sup> Smaller constructs such as scFv, diabodies, triabodies, minibodies, and Fab have been shown in xenograft systems to have shorter half-lives and higher tumor-to-organ ratios, but lower overall tumor uptake at long times compared with corresponding Fab<sub>2</sub> constructs.<sup>53,54</sup> Liu et al.<sup>55</sup> demonstrated superior tumor uptake of an Fab compared with the parent Ab in a xenograft model during a 3–14-hour time window suggesting applicability for imaging, whereas Sundaresan et al.<sup>56</sup> reached similar conclusions for minibodies and diabodies. Holton et al. and Covell et al.<sup>57,58</sup> systematically compared biodistribution of mAbs with the corresponding Fab and Fab<sub>2</sub> constructs, both for binding Abs and nonspecific Abs.

Several groups have examined the effect of increased valence. Adams et al.<sup>5</sup> showed that a diabody possessed significantly improved *in vivo* tumor retention compared with its corresponding scFv monomer. Nielsen et al.<sup>59</sup> created bivalent diabodies from scFv ranging in affinity from 10<sup>-7</sup> to 10<sup>-9</sup> M, targeted to the same epitope. These bivalent diabodies possessed affinities with a much narrower range of 6 × 10<sup>-9</sup> to 3 × 10<sup>-10</sup> M. Tumor retention was improved by conversion to the diabody format, and optimal tumor biodistribution was seen for the weakest-binding diabody, again demonstrating that increases in affinity and avidity beyond the optimum may have little utility. Adams et al.<sup>60</sup> compared scFv dimers with 1 and 2 Ag-specific binding sites to the parent scFv, and showed that the enhanced tumor retention of such dimeric Abs in a murine xenograft model compared with scFv is due to increased valence, not to increased molecular weight. However, both of these constructs are below the 60-kDa glomerular filtration threshold, and thus are consider-

ably smaller than IgG molecules. Rossi et al.<sup>61</sup> show in a xenograft system that tetrabodies have higher tumor uptake than the corresponding triabodies or diabodies. Chauhan et al.<sup>62</sup> compared diabodies and tetrabodies to monovalent scFv in xenografts and found that the multivalent constructs had 3–4-fold higher tumor uptake and 6–8-fold lower renal uptake. In contrast, little difference was seen in the biodistribution between monovalent and divalent constructs of variable domains from camel functional heavy chains.<sup>51</sup> Storto et al.<sup>63</sup> found in patients with hepatic metastases from colorectal cancer that a trivalent Fab<sub>3</sub> construct had comparable tumor uptake and tumor:blood ratios to the parent mAb.

Bivalent Ab constructs may be either monospecific or bispecific. Gruaz-Guyon et al.<sup>64</sup> noted enhanced tumor targeting by bispecific Abs in a pretargeted radioimmunotherapy strategy. Renner et al.<sup>65</sup> found similar biodistribution of a bispecific anti-CD16/anti-CD30 mAb compared with a monospecific anti-CD30 mAb. The bispecific Ab had previously shown a 30% response rate in Hodgkin lymphoma patients resistant to standard therapy.

Clearly, tumor penetration requires sufficient serum exposure. Below we consider factors that influence serum pharmacokinetics.

## Pharmacokinetic Considerations

### Systemic clearance

Because of their large size, IgGs are resistant to filtration by the kidney and urinary elimination is negligible. Ab fragments such as Fab and Fv are sufficiently small to undergo glomerular filtration. However, because of the highly efficient mechanisms for recycling amino acids, the majority of the filtered proteins are reabsorbed rather than passed into the urine. With the exception of IgA (which is subject to a minor extent of biliary excretion), immunoglobulins are generally not eliminated in the feces.<sup>66</sup>

The receptor FcRn (neonatal receptor or *Brambell receptor*), binds to the Fc portion of Abs and plays a major role in clearance of IgG from the circulation.<sup>67,68</sup> FcRn is expressed in cells in close contact with serum. Most serum proteins are pinocytosed and undergo gradual acidification in endosomes, followed by fusion with lysosomes and hydrolysis. However, IgGs bind to FcRn at low pH and the complex is carried back to the cell surface, whereupon it dissociates at neutral pH. FcRn therefore serves as a protective carrier that shuttles IgG away from the lysosome and back into the serum.

Endogenous human IgG<sub>1</sub>, IgG<sub>2</sub>, and IgG<sub>4</sub> all have high affinities for FcRn, and these high affinities largely account for the 3-week circulating half-lives



for these isotypes. Human IgG<sub>3</sub>, which has relatively low affinity for FcRn, has a shorter half-life (1 week). Murine Abs have low affinity for human FcRn and a much shorter serum half-life in humans.<sup>69,70</sup> Mutation of specific amino acids in the C<sub>112</sub> or C<sub>113</sub> domain of Fc alters affinity for FcRn, in turn altering an Ab's serum half-life.<sup>67,71</sup>

Interactions with the target Ag are important to Ab clearance.<sup>72</sup> Many therapeutic Abs demonstrate rapid clearance when their serum concentrations fall below a threshold concentration, corresponding to the point of equal amounts of Ab and target.<sup>73-76</sup>

#### *Volumes of distribution*

After intravenous administration, mAbs initially distribute into a volume roughly equal to the plasma volume (0.045 L/kg)<sup>3,73,76</sup> and on approaching steady state the volume of distribution increases to approximately 0.1 L/kg, reflecting only limited extravascular distribution.<sup>77-79</sup> Biodistribution studies in animals lacking the target Ag have shown that the largest percentage of the dose of mAb is in the plasma and that whole-body distribution predominantly targets organs that are highly perfused with blood.<sup>80-82</sup> In murine xenograft models, mAbs directed against tumor-specific Ags still largely remain in the blood; no more than 20% of the administered dose typically associates with the tumor.<sup>2,83</sup>

The limited extravascular distribution of Abs reflects limited extravasation in normal tissues and elevated interstitial pressure in tumor tissues, as alluded to above. One strategy to promoting vascular penetration into solid tumors exploits surface molecules expressed on tumor vascular endothelia.<sup>84,85</sup> In 1 case, an Ab directed against an endothelial cell surface protein, annexin A1, determined by subtractive proteomics to be specific to solid tumor vascular endothelium, enabled efficient tumor targeting via specialized vascular endothelial structures called caveolae. Caveolae are invaginations of the plasma membrane of endothelial cells, rich in the membrane protein caveolin, through which "transcytosis" of macromolecules from the vascular compartment to the interstitium may occur.<sup>86</sup>

#### *Excretion of novel Ab constructs*

Molecular size of Ab-based molecules is an important determinant of renal excretion. The T<sub>1/2</sub> of a protein molecule correlates with its size relative to the threshold for glomerular filtration, which is estimated to be approximately 60 kDa.<sup>87</sup> Whereas intact IgG molecules (150 kDa) are too large to be filtered by the kidneys, smaller constructs may be subject to extensive renal clearance, resulting in shorter half-

lives. For example; small scFv fragments (30 kDa) have T<sub>1/2</sub> values in the range of 2 hours.<sup>83</sup>

#### *Current Perspectives, Challenges, and Future Directions*

Optimizing biodistribution properties of Ab constructs depends on a large number of host and tumor variables. These include: the density and distribution of target Ag in tumors and normal tissues; the degree of target occupancy and residence time required for tumor cell kill; possible toxicities from normal tissue distribution; tumor size and vascularity; tumor interstitial pressure, convection, and diffusion; and metabolism and internalization rates for Ag-Ab constructs.

An equally large number of Ab construct and therapy variables are available for optimization, including size, charge, and valence; constant region type and glycosylation pattern; presence or absence of a radiolabel or a toxic moiety; dose, route, and schedule of administration; and use of a traditional or of a pretargeting strategy. Given the complexity of the problem, systematic preclinical programs may enhance the likelihood of success in subsequent clinical studies. Such preclinical investigations should integrate both experimental and theoretical approaches.

Preclinical studies of a putative Ab-based therapeutic agent can encompass a variety of constructs, differing in molecular weight, affinity, valence, and/or other features of interest, which bind to the same epitope as demonstrated by competition experiments. The Ag density and target affinities should be known for both tumor cell and cross-reacting normal tissues, and the percent target occupancy and required residence time for tumor cell kill should ideally be estimated *in vitro*. Similarly, rate constants for Ab-Ag internalization should be determined, if applicable. Dose and schedule should be varied and antitumor efficacy, pharmacokinetics, overall biodistribution, homogeneity of intratumoral distribution, and tumor microvessel density and distribution ideally should be measured in tumor-bearing animals with a variety of tumor sizes. Many of these features have been present in the work reviewed above, and they have shed light not only on specific applications but also on general principles.

Studies in tumor-bearing rodents are often confounded by lack of normal tissue reactivity with Ab constructs directed toward human Ags, but studies in transgenic animals can be performed in some instances to alleviate this issue. For example, CEA-transgenic mice were used to test anti-CEA mAbs and revealed specific accumulation in normal gastrointestinal mucosa as well as in adenomas and tumors.<sup>88,89</sup>

Theoretical models may help to understand and interpret experimental results, to prioritize further experimental work, and to translate experiments in murine systems to humans. Baxter et al.<sup>90,91</sup> developed a physiologically based pharmacokinetic model that included tumor, interstitial, plasma, and a variety of organ compartments. The model accounted for transcapillary transport and specific and nonspecific binding, but not for heterogeneity of tumor biodistribution. Adjustable parameters were determined from work with a nonspecific IgG and then carried over to specific Ab constructs with good agreement with experimental data in mice. Importantly, it was feasible to scale up the predictions from mouse to human, taking some adjustable parameters from the literature, other parameters directly from the mouse, and others from the mouse by allometric scaling. Agreement with human data was qualitatively good for a variety of Ab constructs, although the largest discrepancies involved distribution into the tumor.

In optimizing Ag-Ab constructs for affinity and other properties it is well to bear in mind the mechanism of cell kill, and the requirements in terms of percent occupancy of target sites and residence times required to effect killing. If a high percentage occupancy and long residence time are required for cell kill, high affinity may be preferable and the approach would have to be to treat the outer layer of the tumor with each course, "peeling the onion" step by step. Tumors are genetically unstable, however, and if antibody therapies take too long to penetrate them, may acquire resistance.<sup>92</sup> Conjugates of Abs with toxins or chemotherapy must have a sufficient residence time to internalize, but depending on the potency of the toxin or chemotherapy, may require that residence time for only a small percentage of receptors. When only brief residence time or low percentage occupancy is required for cell kill, a lower-affinity Ab might enhance uniformity of tumor penetration. Radioimmunotherapy is a special case in that only a brief residence time may be required but the path length of the radiation may enhance the effective tumor penetration. Similarly, Abs which bind to circulating soluble factors, to the vascular endothelium, to the extracellular matrix, or to immune effector cells, may not need to penetrate the tumor to the same extent.

In summary, we suggest the following algorithm, supported in each case by preclinical experimental and theoretical studies, and if possible clinical biodistribution studies, when designing an Ab construct and dosing schedule:

1. Determine the extent of tumor penetration that is required, considering whether the target is on the tumor

cell surface, on the extracellular matrix, on immune effector cells, or on circulating factors, and to what extent its effect is extended by bystander effects or radiation path-length if the antibody is to be radiolabeled. Radiolabeled antibodies and those acting on circulating factors or immune complexes may not need to penetrate tumors to the same extent. The answer to this question determines the applicability of Questions 3 and 4.

2. Determine the extent and duration of receptor occupancy that are required to achieve the desired pharmacodynamic effects. The affinity or avidity for the target must be sufficient to achieve this goal, irrespective of other considerations. Once this minimal affinity is achieved, further increases in affinity must be balanced against possible reductions in homogeneous tumor penetration. These considerations apply in settings of Ag excess. If Ab excess can be achieved, all binding sites can be saturated. Determining whether the situation reflects Ag excess or Ab excess requires knowledge of the target density on tumor and other cells as well as the pharmacokinetics of the Ab. Radiolabeled antibodies may require much lower receptor occupancy in that they can achieve cytotoxicity at a distance determined by their radiation pathlength.

3. Ab constructs should have isoelectric points near physiologic pH if they are required to diffuse through the extracellular matrix or penetrate into tumors (see Question 1), as molecules with neutral charge diffuse more readily.

4. If tumor penetration is required (see Question 1), consider smaller Ab constructs that diffuse more readily into the tumor, enhancing their tumor-specific retention by increasing their valence, as may be achieved with such constructs as diabodies. Smaller constructs that are below the 60-kDa threshold for glomerular filtration will be more rapidly excreted if they are not retained in the tumor, particularly if they do not have an Fc portion enabling recycling through the FcRn receptor. As long as tumor retention is sufficient, however, rapid excretion may lead to reduced normal tissue binding, and hence reduced toxicity.

These principles should prove useful in guiding the development of Abs for cancer therapy.

## REFERENCES

1. Adams GP, Weiner LM. Monoclonal antibody therapy of cancer. *Nat Biotechnol*. 2005;23:1147-1157.
2. Sedlacek HH, Seemann G, Hoffmann D, et al. Antibodies as carriers of cytotoxicity. In: Huber H, Queiber W, editors. *Contributions to Oncology*. Basel: Karger, 1992.
3. Adams CW, Allison DE, Flagella K, et al. Humanization of a recombinant monoclonal antibody to produce a therapeutic HER dimerization inhibitor, pertuzumab. *Cancer Immunol Immunother*. 2006;55:717-727.
4. Adams GP, Schier R, McCall AM, et al. High affinity restricts the localization and tumor penetration of single-chain Fv antibody molecules. *Cancer Res*. 2001;61:4750.

5. Adams GP, Schier R, McCall AM, et al. Prolonged in vivo tumour retention of a human diabody targeting the extracellular domain of human HER2/neu. *Br J Cancer*. 1998; 77:1405-1412.
6. Albrecht H, Burke PA, Natarajan A, et al. Production of soluble ScFvs with C-terminal-free thiol for site-specific conjugation or stable dimeric ScFvs on demand. *Bioconjug Chem*. 2004;15:16-26.
7. Kim SJ, Park Y, Hong HJ. Antibody engineering for the development of therapeutic antibodies. *Mol Cell*. 2005;20:17-29.
8. Perisic O, Webb PA, Holliger P, Winter G, Williams RL. Crystal structure of a diabody, a divalent antibody fragment. *Structure*. 1994;2:1217-1228.
9. Hu S, Shively L, Raubitschek A, et al. Minibody: a novel engineered anti-carcinoembryonic antigen antibody fragment (single-chain Fv-CH3) which exhibits rapid, high-level targeting of xenografts. *Cancer Res*. 1996;56:3055-3061.
10. Schaedel O, Reiter Y. Antibodies and their fragments as anti-cancer agents. *Curr Pharm Des*. 2006;12:363-378.
11. Tunggal JK, Cowan DS, Shaikh H, Tannock IF. Penetration of anticancer drugs through solid tissue: a factor that limits the effectiveness of chemotherapy for solid tumors. *Clin Cancer Res*. 1999;5:1593-1596.
12. Jang SH, Wientjes MG, Lu D, Au JL. Drug delivery and transport to solid tumors. *Pharm Res*. 2003;20:1337-1350.
13. Netti PA, Berk DA, Swartz MA, Grodzinsky AJ, Jain RK. Role of extracellular matrix assembly in interstitial transport in solid tumors. *Cancer Res*. 2000;60:2497-2503.
14. Thiagarajah JR, Kim JK, Magzoub M, Verkman AS. Slowed diffusion in tumors revealed by microfiber-optic epifluorescence photobleaching. *Nat Methods*. 2006;3:275-280.
15. Pluen A, Boucher Y, Ramanujan S, et al. Role of tumor-host interactions in interstitial diffusion of macromolecules: cranial vs. subcutaneous tumors. *Proc Natl Acad Sci U S A*. 2001;98:4628-4633.
16. Znati CA, Rosenstein M, McKee TD, et al. Irradiation reduces interstitial fluid transport and increases the collagen content in tumors. *Clin Cancer Res*. 2003;9:5508-5513.
17. Tannock IF, Steel GG. Quantitative techniques for study of the anatomy and function of small blood vessels in tumors. *J Natl Cancer Inst*. 1969;42:771-782.
18. Heuser LS, Miller FN. Differential macromolecular leakage from the vasculature of tumors. *Cancer Immunol Immunother*. 1986;35:461-464.
19. Jain RK. Physiological barriers to delivery of monoclonal antibodies and other macromolecules in tumors. *Cancer Res*. 1990;50(3 Suppl):814s-819s.
20. Nugent LJ, Jain RK. Extravascular diffusion in normal and neoplastic tissues. *Cancer Res*. 1984;44:238-244.
21. Gerlowski LE, Jain RK. Microvascular permeability of normal and neoplastic tissues. *Microvasc Res*. 1986;31:288-308.
22. Clauss MA, Jain RK. Interstitial transport of rabbit and sheep antibodies in normal and neoplastic tissues. *Cancer Res*. 1990;50:3487-3492.
23. Jain RK, Baxter LT. Mechanisms of heterogeneous distribution of monoclonal antibodies and other macromolecules in tumors: significance of elevated interstitial pressure. *Cancer Res*. 1988;48:7022-7032.
24. Maeda H, Wu J, Sawa T, Matsumura Y, Hori K. Tumor vascular permeability and the EPR effect in macromolecular therapeutics: a review. *J Control Release*. 2000;65:271-284.
25. Baxter LT, Jain RK. Transport of fluid and macromolecules in tumors. I. Role of interstitial pressure and convection. *Microvasc Res*. 1989;37:77-104.
26. Boucher Y, Baxter LT, Jain RK. Interstitial pressure gradients in tissue-isolated and subcutaneous tumors: implications for therapy. *Cancer Res*. 1990;50:4478-4484.
27. Roh HD, Boucher Y, Kalnicki S, et al. Interstitial hypertension in carcinoma of uterine cervix in patients: possible correlation with tumor oxygenation and radiation response. *Cancer Res*. 1991;51:6695-6698.
28. Gutmann R, Leunig M, Feyh J, et al. Interstitial hypertension in head and neck tumors in patients: correlation with tumor size. *Cancer Res*. 1991;52:1993-1995.
29. Less JR, Posner MC, Boucher Y, et al. Interstitial hypertension in human breast and colorectal tumors. *Cancer Res*. 1992;52:6371-6374.
30. Williams LE. Uptake of radiolabelled anti-CEA antibodies in human colorectal primary tumors as a function of tumor mass. *Eur J Nucl Med*. 1993;20:345.
31. Graff CP, Wittrup KD. Theoretical analysis of antibody targeting of tumor spheroids: importance of dosage for penetration, and affinity for retention. *Cancer Res*. 2003;63:1288-1296.
32. Colcher D, Pavlinkova G, Beresford G, et al. Pharmacokinetics and biodistribution of genetically-engineered antibodies. *Q J Nucl Med*. 1998;42:225-241.
33. Melkko S, Halin C, Borsi L, Zardi L, Neri D. An antibody-calmodulin fusion protein reveals a functional dependence between macromolecular isoelectric point and tumor targeting performance. *Int J Radiat Oncol Biol Phys*. 2002;54:1485-1490.
34. Weinstein JN, van Osdol W. Early intervention in cancer using monoclonal antibodies and other biological ligands: micropharmacology and the "binding site barrier." *Cancer Res*. 1992;52(9 Suppl):2747a-2751s.
35. Fujimori K, Covell DG, Fletcher JE, Weinstein JN. A modeling analysis of monoclonal antibody percolation through tumors: a binding-site barrier. *J Nucl Med*. 1990;31:1191-1198.
36. Posey JA, Khazaeli MB, DeGrosso A, et al. A pilot trial of Vitaxin, a humanized anti-vitronectin receptor (anti alpha v beta 3) antibody in patients with metastatic cancer. *Cancer Biother Radiopharm*. 2001;16:125-132.
37. Kwok CS, Cole SE, Liao SK. Uptake kinetics of monoclonal antibodies by human malignant melanoma multi-cell spheroids. *Cancer Res*. 1988;48:1856-1863.
38. Olabiran Y, Ledermann JA, Marston NJ, et al. The selection of antibodies for targeted therapy of small-cell lung cancer (SCLC) using a human tumor spheroid model to compare the uptake of cluster I and cluster w4 antibodies. *Br J Cancer*. 1994;69:247-252.
39. Langmuir VK, Mendonca HL, Woo DV. Comparisons between two monoclonal antibodies that bind to the same antigen but have different affinities: uptake kinetics and 125I-antibody therapy efficacy in multi-cellular spheroids. *Cancer Res*. 1992;52:4728-4734.
40. Hjelsten MH, Rasch-Halvorsen K, Brekken C, Bruland O, de L Davies C. Penetration and binding of monoclonal antibody in human osteosarcoma multi-cell spheroids. Comparison of confocal laser scanning microscopy and autoradiography. *Acta Oncol*. 1996;35:273-279.
41. Myrdal S, Foster M. Time-resolved confocal analysis of antibody penetration into living, solid tumor spheroids. *Scanning*. 1994;16:155-167.

42. Ballangrud AM, Yang WH, Charlton DE. Response of LNCaP spheroids after treatment with an  $\alpha$ -particle emitter (213Bi)-labeled anti-prostate specific membrane antigen antibody (1591). *Cancer Res*. 2001;61:2008-2014.
43. Kuan CT, Wikstrand CJ, Archer G. Increased binding affinity enhances targeting of glioma xenografts by EGFRvIII-specific scFv. *Int J Cancer*. 2000;2:21-36.
44. Wu AM, Chen W, Raubitschek A. Tumor localization of anti-CEA single-chain Fvs: improved targeting by non-covalent dimers. *Immunotechnology*. 1996;2:21-36.
45. Cooke SP, Pedley RB, Boden R, Begent RH, Chester KA. In vivo tumor delivery of a recombinant single-chain Fv: tumor necrosis factor: a fusion protein. *Bioconjug Chem*. 2002;13:7-15.
46. Baxter LT, Jain RK. Transport of fluid and macromolecules in tumors. IV. A microscopic model of the perivascular distribution. *Microvasc Res*. 1991;41:252-272.
47. Blumenthal RD. The effect of antibody protein dose on the uniformity of tumor distribution of radioantibodies: an autoradiographic study. *Cancer Immunol Immunother*. 1991;33:351.
48. Weiner LM. Improving the tumor selective delivery of single-chain Fv molecules. *Tumor Target*. 1995;1:51.
49. Verel I, Heider KF, Siegmund M, et al. Tumor targeting of antibodies with different affinity for target antigen CD44V6 in nude mice bearing head and neck cancer xenografts. *Int J Cancer*. 2002;99:396-402.
50. Yokota T, Milenic DE, Whitlow M, Schlom J. Rapid tumor penetration of a single-chain Fv and comparison with other immunoglobulin forms. *Cancer Res*. 1992;52:3402-3408.
51. Pang J, Jin HB, Song JD. Construction, expression and tumor targeting of a single-chain Fv against human colorectal carcinoma. *World J Gastroenterol*. 2003;9:726-730.
52. Cortez-Retamozo V. Efficient tumor targeting by single-domain antibody fragments of camels. *Int J Cancer*. 2002;98:456-462.
53. Tahris K, Fook-Thean L, Smyth FE, et al. Biodistribution properties of (111)-indium-labeled C-functionalized trans-cyclohexyl diethylenetriaminepentaacetic acid humanized 3S193 diabody and F(ab')(2) constructs in a breast carcinoma xenograft model. *Clin Cancer Res*. 2001;7:1061-1072.
54. Khawli LA, Biela B, Hu P, Epstein AL. Comparison of recombinant derivatives of chimeric TNT-3 Ab for the radioimaging of solid tumors. *Hybrid Hybridomics*. 2003;22:1-9.
55. Liu N, Jin J, Zhang S, et al. At labeling of a monoclonal antibody and its Fab fragment: cytotoxicity on human gastric cancer cells and biodistribution in nude mice with tumor xenografts. *J Radioanal Nuclear Chem*. 2001;247:129-133.
56. Sundaresan G, Yazaki PJ, Shively JE, et al. 124I-labeled engineered anti-CEA minibodies and diabodies allow high-contrast, antigen-specific small-animal PET imaging of xenografts in athymic mice. *J Nucl Med*. 2003;44:1962-1969.
57. Holton OD 3d, Black CD, Parker RJ, et al. Biodistribution of monoclonal IgG1, F(ab')2, and Fab' in mice after intravenous injection. Comparison between anti-B cell (anti-Ly6.2) and irrelevant (MOPC-21) antibodies. *J Immunol*. 1987;139:3041-3049.
58. Covell DG, Barbet J, Holton OD, et al. Pharmacokinetics of monoclonal immunoglobulin G1, F(ab')2, and Fab' in mice. *Cancer Res*. 1986;46:6434-6440.
59. Nielsen UB, Adams GP, Weiner LM, Marks JD. Targeting of bivalent anti-ErbB2 diabody antibody fragments to tumor cells is independent of the intrinsic antibody affinity. *Cancer Res*. 2000;60:6434-6440.
60. Adams GP, Tai MS, McCartney JB, et al. Avidity-mediated enhancement of in-vivo tumor targeting by single-chain Fv dimers. *Clin Cancer Res*. 2006;12:1599-1605.
61. Rossi EA, Chang CH, Karacay H, et al. Tumor targeting with humanized anti-CEA diabodies, triabodies, and tetrabodies. *Proc Am Assoc Cancer Res*. [Meeting 911] 2002;43:93.
62. Chauhan SC, Jain M, Moore ED, Baranowska-Kortylewicz J, Batra SK. Pharmacokinetics and biodistribution of 177Lu-labeled multivalent single chain Fv constructs of the pancreatic carcinoma monoclonal antibody CC49. *Proc Am Assoc Cancer Res*. [Meeting 171] 2003;94.
63. Storto G, Buchegger R, Waibel R, et al. Biokinetics of a F(ab')3 iodine-131 labeled Ag binding construct (Mab 35) directed against CEA in patients with colorectal carcinoma. *Cancer Biother Radiopharm*. 2001;16:371-379.
64. Gruaz-Guyon A, Janevik-Ivanovska E, Raguin O, De Labriolle-Vaylet C, Barbet J. Radio-labeled bivalent haptens for tumor immunodetection and radioimmunotherapy. *Q J Nucl Med*. 2001;45:201-206.
65. Renner C, Stehle I, Lee FT, et al. Targeting properties of an anti-CD16/anti-CD30 bispecific antibody in an in vivo system. *Cancer Immunol Immunother*. 2001;50:102-108.
66. Delacroix DL, Hodgson HJ, McPherson A, Dive C, Vaerman JP. Selective transport of polymeric immunoglobulin A in bile. Quantitative relationships of monomeric and polymeric immunoglobulin A, immunoglobulin M, and other proteins in serum, bile, and saliva. *J Clin Invest*. 1982;70:230-241.
67. RP Junghans. Finally! The Brambell receptor (FcRn). Mediator of transmission of immunity and protection from catabolism for IgG. *Immunol Res*. 1997;16:27-57.
68. Lobo ED, Hansen RJ, Balthasar JP. Antibody pharmacokinetics and pharmacodynamics. *J Pharm Sci*. 2004;93:2645-2668.
69. Zhou J, Johnson JE, Ghetie V, Ober RJ, Ward ES. Generation of mutated variants of the human form of the MHC class I-related receptor, FcRn, with increased affinity for mouse immunoglobulin G. *J Mol Biol*. 2003;332:901-913.
70. Ober RJ, Radu CG, Ghetie V, Ward ES. Differences in promiscuity for antibody-FcRn interactions across species: implications for therapeutic antibodies. *Int Immunol*. 2001;13:1551-1559.
71. Shields RL, Namenuk AK, Hong K, et al. High resolution mapping of the binding site on human IgG1 for Fc gamma RI, Fc gamma RII, Fc gamma RIII, and FcRn and design of IgG1 variants with improved binding to the Fc gamma R. *J Biol Chem*. 2001;276:6591-6604.
72. Ternant D, Ohresser M, Cecile T, et al. Dose-response relationship and pharmacogenetics of Anti-RhD monoclonal antibodies. *Blood*. 2005;106:1503-1504.
73. Dowling TC, Chavaille PA, Young DG, et al. Phase 1 safety and pharmacokinetic study of chimeric murine-human monoclonal antibody c alpha Sx2 administered intravenously to healthy adult volunteers. *Antimicrob Agents Chemother*. 2005;49:1808-1812.
74. Rowinsky EK, Schwartz GH, Gollob JA, et al. Safety, pharmacokinetics, and activity of ABX-EGF, a fully human anti-epidermal growth factor receptor monoclonal antibody in patients with metastatic renal cell cancer. *J Clin Oncol*. 2004;22:3003-3015.

75. Kloft C, Graefe EU, Taniswell P, et al. Population pharmacokinetics of sibrotuzumab, a novel therapeutic monoclonal antibody, in cancer patients. *Invest New Drugs*. 2004;22: 39-52.
76. de Bono JS, Tolcher AW, Forero A, et al. ING-1, a monoclonal antibody targeting Ep-CAM in patients with advanced adenocarcinomas. *Clin Cancer Res*. 2004;10:7555-7566.
77. Trang JM, LoBuglio AF, Wheeler RH, et al. Pharmacokinetics of a mouse/human chimeric monoclonal antibody (C-17-1A) in metastatic adenocarcinoma patients. *Pharm Res*. 1990;7:587-592.
78. Trang JM. Pharmacokinetics and metabolism of therapeutic and diagnostic antibodies. In: Ferraiolo BL, Mohler MA, Gloff CA, editors. *Protein Pharmacokinetics and Metabolism*. New York: Plenum Press; 1992:223-270.
79. Chow FS, Benincosa LJ, Wilson SB, et al. Pharmacokinetic and pharmacodynamic modeling of humanized anti-factor IX antibody (SB 249417) in humans. *Clin Pharmacol Ther*. 2002;71:235-345.
80. Arizono H, Ishii S, Nagao T, et al. Pharmacokinetics of a new human monoclonal antibody against cytomegalovirus. First communication: plasma concentration, distribution, metabolism and excretion of the new monoclonal antibody, regavirumab after intravenous administration in rats and rabbits. *Arzneimittelforschung*. 1994;44:890-898.
81. Fox JA, Hotaling TE, Struble C, et al. Tissue distribution and complex formation with IgE of an anti-IgE antibody after intravenous administration in cynomolgus monkeys. *J Pharmacol Exp Ther*. 1996;279:1000-1008.
82. Lin YS, Nguyen C, Mendoza JL, et al. Preclinical pharmacokinetics, interspecies scaling, and tissue distribution of a humanized monoclonal antibody against vascular endothelial growth factor. *J Pharmacol Exp Ther*. 1999;288:371-378.
83. Holliger P, Hudson PJ. Engineered antibody fragments and the rise of single domains. *Nat Biotechnol*. 2005;23:1126-1136.
84. Contag CH, Bachmann MH. Molecular medicine: the writing is on the vessel wall. *Nature*. 2004;429:618-619.
85. Durr E, Yu J, Krasinska KM, et al. Direct proteomic mapping of the lung microvascular endothelial cell surface in vivo and in cell culture. *Nat Biotechnol*. 2004;22:985-992.
86. Oh P, Li Y, Yu J, et al. Subtractive proteomic mapping of the endothelial surface in lung and solid tumours for tissue-specific therapy. *Nature*. 2004;429:629-635.
87. Reff ME, Hariharan K, Braslawsky G. Future of monoclonal antibodies in the treatment of hematologic malignancies. *Cancer Control*. 2002;9:152-166.
88. Wilkinson RW, Ellison D, Poulson R. Assessment of preclinical models for colorectal cancer. *Br J Cancer*. 2001;85(Suppl 1):39.
89. Wilkinson RW, Ross EL, Poulson R, et al. Antibody targeting studies in a transgenic murine model of spontaneous colorectal tumors. *Int Proc Natl Acad Sci U S A*. 2001;98:10256-10260.
90. Baxter LT, Zhu H, Mackensen DG, Jain RK. Physiologically based pharmacokinetic model for specific and nonspecific monoclonal antibodies and fragments in normal tissues and human tumor xenografts in nude mice. *Cancer Res*. 1994;54:1517-1512.
91. Baxter LT, Zhu H, Mackensen DG, Butler WF, Jain RK. Biodistribution of monoclonal antibodies: scale-up from mouse to human using a physiologically based pharmacokinetic model. *Cancer Res*. 1995;55:4611-4622.
92. Beckman RA, Loeb LA. Genetic instability in cancer: theory and experiment. *Semin Cancer Biol*. 2005;15:423-435.

# Production technologies for monoclonal antibodies and their fragments

Dana C Andersen\* and Dorothea E Reilly

In recent years, monoclonal antibodies have emerged as an increasingly important class of human therapeutics. A variety of forms of antibodies, including fragments such as Fabs, Fab'<sub>2</sub>s and single-chain Fvs, are also being evaluated for a range of different purposes. A variety of expression systems and improvements within these systems have been developed to address these growing and diverse needs.

## Addresses

Genentech, Inc., 1 DNA Way, South San Francisco, CA 94080, USA  
\*e-mail: andersen.dana@gene.com

Current Opinion in Biotechnology 2004, 15:456-462

This review comes from a themed issue on  
Biochemical engineering

Edited by Manuel Carrondo and John G. Aunins

Available online 25th August 2004

0958-1669/\$ - see front matter

© 2004 Elsevier Ltd. All rights reserved.

DOI: 10.1016/j.copbio.2004.08.002

## Abbreviations

ADCC antibody-dependent cellular cytotoxicity  
CHO Chinese hamster ovary  
DHFR dihydrofolate reductase  
IgG immunoglobulin G  
PEG polyethylene glycol

## Introduction

Several recent successful clinical results have led to an increased interest in approaches for expressing various forms of monoclonal antibodies. Large doses are often required for therapeutic purposes, in some cases exceeding a gram per patient per year. This need has driven the development of a variety of production systems to make these molecules efficiently and cost-effectively. Truncated forms of antibodies, including Fab, Fab'<sub>2</sub> and single-chain Fv forms, have also been used for a variety of clinical applications. Depending on the specific use, different forms and different production hosts might be desirable and several recent reviews have specifically addressed issues surrounding production in microbial systems [1,2] and transgenic plants [3], as well as general production issues [4]. Given the rapid pace of progress and large amount of active work in this field, this review will necessarily be incomplete and will focus on a subset of the most recently reported advances and developments

in expression technologies for antibodies and antibody fragments.

## Antibody fragments and microbial production

Antibody fragments such as Fabs or Fab'<sub>2</sub>s can be the therapeutic of choice for some applications where Fc-mediated effector functions are either not required or are deleterious. The smaller antibody fragments exhibit a shorter circulating half-life than full-length immunoglobulin G (IgG) molecules, but their smaller size can also make them more suitable for applications such as tumor penetration and imaging [4].

These antibody fragments can be generated from mammalian-produced full-length antibodies by treating the IgGs with pepsin or papain. However, *Escherichia coli* remains the production system of choice for antibody fragments used in therapeutic applications for several reasons. Firstly, *E. coli* production can offer a rapid means to progress from antibody selection to good manufacturing practice (GMP) production of antibodies, due to the ease and speed of making productive cell lines compared to eukaryotic cell lines [1]. Secondly, as will be discussed below, high production levels of antibody fragments are usually attainable when *E. coli* is used as the production organism. Currently, there are several Fabs or Fab's in clinical trials (Genentech <http://www.gene.com> and Celltech <http://www.celltech.com>) produced using *E. coli*.

A variety of approaches have been adopted by different groups to improve the production levels of antibody fragments using the *E. coli* system. Expression levels of up to 2 g/L have been reported [5]. The approaches taken include optimizing the expression of light and heavy chains to obtain increased titers of a Fab' [6], host-cell engineering to prevent proteolysis of the light chain [5], and co-expressing chaperones to improve protein folding [7] or disulfide bond formation [8].

Although the short circulating half-life of antibody fragments is suitable for some applications such as tumor imaging, it can also be a limitation for a wider range of therapeutic uses. Chapman showed that site-specific attachment of either a single or a double 25 kDa or a single 40 kDa polyethylene glycol (PEG) moiety to an Fab' could increase the circulating half-life by up to 80% of that seen for the IgG without a loss in antigen binding [9]. Leong *et al.* showed that the circulating half-life of an Fab' could be modulated by the choice of size and

structure of the PEG moiety attached [10]. A recent review by Chapman further discusses the increases in circulating half-life that can be obtained by attaching PEG moieties to antibodies [11]. Dennis *et al.* describe an albumin-binding peptide that they fused to the C terminus of a Fab light chain. Using this peptide they were able to demonstrate a 26- to 37-fold increase in circulating half-life in either mice or rabbits [12\*\*]. The development of such techniques to increase the circulating half-life can extend the therapeutic usefulness of antibody fragments and allows for less frequent patient dosing.

There has also been a recent report of producing full-length antibodies in *E. coli* [13\*\*]. Up until this report, the dogma had been that it was too difficult to make Fc-containing antibodies in *E. coli*. The full-length antibodies produced in *E. coli* are aglycosylated and lack the ability to bind to the various Fc $\gamma$  receptors, but they do retain binding to the neonatal Fc receptor (FcRn) and, thus, have a long circulating half-life. Although many therapeutic uses of antibodies are thought to require the effector functions mediated through Fc $\gamma$  receptors, there are also therapeutic indications such as the binding of a soluble antigen that do not require effector functions. Aglycosylated antibodies can be a suitable choice for these types of indications.

### Fungal production

There have been recent reports describing the use of *Aspergillus niger* for the production of monoclonal antibodies or antibody fragments. Fungal production of antibodies could offer potential advantages over *E. coli*, if production titers can be boosted in the fungal systems. Antibodies and fragments produced in the *E. coli* system are usually retained in the *E. coli* periplasm, necessitating some type of cell lysis and recovery of the antibody of interest from a complex protein milieu. Proteins made in fungal systems are generally secreted to the culture supernatant, a potential advantage for product purification. Filamentous fungi such as *Aspergillus* are capable of secreting high levels of homologous proteins, but these high levels have yet to be obtained with heterologous proteins [14].

Ward *et al.* expressed full-length IgGs in *A. niger* using an N-terminal fusion to glucoamylase for both light and heavy chains. They relied on the endogenous KexB protease in *A. niger* to cleave off the fusion during the secretion of the antibody [15\*]. The authors found inefficient cleavage of glucoamylase from the antibody, but were able to partially remedy the problem with the addition of glycine residues between the glucoamylase and either the light chain or heavy chain sequence. The resulting antibody was found to have glycine residues at the N terminus of the two chains. Expression levels of up to 900 mg/L are reported.

An outstanding question concerning antibody production in fungal systems is whether the differences in glycosylation compared with mammalian systems will cause immune responses or lead to a lack of effector functions in therapeutic uses. The antibodies made in *A. niger* were found to contain a mixture of glycosylated and aglycosylated heavy chains, but did demonstrate a long circulating half-life and antibody-dependent cellular cytotoxicity (ADCC).

An interesting new approach to modifying the glycans attached to recombinant proteins made in fungal systems was recently described by Hamilton *et al.* [16\*\*]. They used a combinatorial library to optimize the cloning of various glycotransferases to humanize the glycosylation pathway of *Pichia pastoris*. If this approach can be combined with high-level expression of antibodies (up to 1.2 g/L has been reported [17]), it could compete with existing mammalian culture systems for the production of antibodies that retain effector functions and have human-like glycosylation. In another recent study, monomeric scFv production in *P. pastoris* was also demonstrated and optimized [18].

### Plant production

Research has continued into using plants as a production platform for antibodies and other therapeutic proteins. A recent review [3] discusses the current state of progress and the outstanding issues that need to be resolved in order for a plant-derived antibody for parental delivery to be approved for marketing. The potential advantages for the plant system that are often cited are capital cost savings, the ability to either increase or decrease production output depending on market needs, and the lack of mammalian pathogens in plants. Some of the current hurdles include a long initial lead time for production, regulatory uncertainties, and questions about the suitability of plant glycans for human therapeutics. One approach has been to mutate the N-linked glycosylation site found in the Fc of monoclonal antibodies and to thereby produce an aglycosylated antibody. Another approach taken has been to try and modify the glycosylation enzymes in plants to more closely resemble those in humans. Bakker *et al.* co-expressed human  $\beta$ 1,4-galactosyltransferase and an antibody in tobacco plants and obtained a galactosylation profile resembling that found in mammalian antibodies [19].

### Mammalian cell production

While specific types of antibodies and antibody fragments are amenable to production in microbial or other systems, mammalian cells remain the dominant system for the production of the majority of full-length therapeutic antibodies. Recombinant Chinese hamster ovary (CHO) and NS0 cells remain the most prominent cell lines of choice, although numerous other cell lines have been explored as well. For example, the human cell line

PER.C6 has recently been demonstrated to produce significant levels of recombinant products including antibodies in serum-free, suspension cultures [20,21].

### Cell line development

The generation of stable cell lines that produce high levels of product is certainly one of the most critical elements required for the development of an efficient cell culture process. The use of dihydrofolate reductase (DHFR) as a marker for selection and amplification using methotrexate represents the most common system for generating cells with high expression in CHO cells. In a recent modification of this standard approach, Bianchi and McGrew divided DHFR into two fragments that could re-associate, aided by a leucine zipper, into an active molecule [22]. The two pieces could then be inserted into the expression vector adjacent to light and heavy chains, respectively, to increase the probability that only amplification events that amplified both the heavy and light chain segments would be selected. Several groups have also identified flanking elements to include in vectors for the purpose of increasing the development of stable, high-producing clones, such as the recently reported example of expression augmenting sequence elements (EASE) [23] (reviewed in [24–26]).

The most commonly used approaches for transfection with random integration also lead to a wide diversity of expression levels (e.g. see [27]). Recent approaches to screen through this diversity in a high-throughput manner include approaches based on fluorescence-activated cell sorting (FACS) using a labeled anti-Fc antibody [28], a metallothionein green fluorescent protein (GFP) fusion [29] or a surface affinity matrix [30].

### Cellular engineering

A recent trend has been the development of additional genetic manipulations to antibody-producing cell lines to confer properties enabling improved bioreactor performance. Specifically, manipulations have been directed primarily at controlling cell growth, preventing cell death or influencing folding and glycosylation.

Over the past decade, a variety of approaches have been developed and evaluated to enable growth control with the goal of decoupling growth and recombinant protein production (reviewed in [25]). A recent example is the use of inducible expression of p27 to induce growth arrest in a serum-free recombinant CHO culture [31]. Another study correlated the increased productivity observed in p27-arrested CHO cultures with increased cell energy usage [32]. Bi *et al.* also recently reported that specific antibody expression was increased approximately fourfold in an NS0 culture arrested using p21 overexpression [33]. Non-genetic approaches for growth control with sustained protein production, which hold the potential advantage of being easier to implement for existing cell culture

processes, have also been reported in CHO systems through the use of galactose in place of glucose as a carbon source [34] or the use of nucleosides such as adenosine [35]. Finally, an approach using FACS-sorting of GFP-expressing cells was used to isolate protein-producing CHO cells in a growth-arrested state [36].

Apoptosis can be the major mechanism for cellular death in fed-batch cell culture. Consequently, several different approaches have been recently evaluated to prolong culture viability and, potentially, increase product titers. Members of the Bcl family, specifically *bcl-2* and *bcl-x<sub>L</sub>*, have represented the most common elements for engineering apoptosis resistance (see [37]), although recent studies have also demonstrated effects using Aven [38], XIAP and CrmA [39] and approaches targeting Caspase-3 at the RNA level have been reported [40]. Another study showed a modest benefit of hsp70 overexpression on NS0 apoptosis-resistance and on the productivity of hybridoma cells generated from these hosts [41]. Following earlier work in which Bcl-2 expression was shown to improve antibody and recombinant protein expression in the presence of butyrate in CHO cultures, an apoptosis-resistant, DHFR- and Bcl-2 overexpressing host was recently created by Lee and Lee [42]. In one recent study, the relative merits of Bcl-2 and Bcl-x<sub>L</sub> were evaluated using a serum-free CHO-DG44 line producing a soluble intercellular adhesion molecule. In this analysis, Bcl-x<sub>L</sub> was observed to have more potent apoptosis-resistance effects, although benefits on total recombinant protein expression were only observed after amplifying the Bcl-x<sub>L</sub> expression to relatively high levels [43]. In response to potential concerns about the long-term effects of Bcl-x<sub>L</sub> overexpression, another group recently developed an inducible system, using the metallothionein promoter, for Bcl-x<sub>L</sub> expression and apoptosis-resistance during the production phase of hybridoma cultures [44]. Finally, the combination of growth control and anti-apoptosis effects via genetic engineering was recently evaluated in perfusion NS0 cultures using combined p21 and Bcl-2 overexpression and enabled antibody specific productivities approaching 50 pg/cell/day [45].

In addition to growth control and apoptosis, limitations in the secretory pathway represent a third target for cellular engineering approaches. For example, one recent study evaluated the levels of three potentially important secretory pathway proteins, heavy chain binding protein (BiP), glucose regulated protein 94 (GRP94) and protein disulfide isomerase (PDI), in hybridomas grown in serum-containing and serum-free medium and found a correlation between GRP94 and PDI levels and monoclonal antibody production rates [46]. In another study, calnexin and calreticulin overexpression were found to nearly double the specific productivity of thrombopoietin in recombinant CHO cultures [47].



A variety of approaches have been demonstrated for engineering the glycosylation pathway to manipulate the characteristics of antibodies mediated by oligosaccharides (reviewed by [24,48,49]). Recent studies have demonstrated that the absence of fucose can dramatically increase ADCC [50,51]. As previously described for plant cultures, an alternative approach is to engineer the antibody sequence to manipulate effector functions (reviewed by [52]). In another recent study, Fc sequence changes were identified to increase serum half-life as well [53].

### Process conditions

As monoclonal antibody production processes are increasingly scaled to larger fermentor volumes to meet increasing commercial demands, traditional scale-up issues may present new challenges. For example, a recent study using NS0 cultures explored the effects of pH perturbations, which can occur in large fermentors as a consequence of base addition for pH control [54]. Depending on the fermentor configuration, elevated carbon dioxide levels can also become an issue at larger scales. Carbon dioxide could have direct effects on cell metabolism or could affect culture performance by more general mechanisms related to the increased osmolality resulting from increased carbon dioxide levels. To distinguish between these potential mechanisms, carbon dioxide and osmolality were independently manipulated in hybridoma cultures and revealed an increase in productivity with increased osmolality, while carbon dioxide alone inhibited productivity [55]. Additionally, galactosylation of a hybridoma-produced IgG2a decreased with elevated osmolality, while it increased with elevated carbon dioxide levels (and controlled osmolality) [56]. Certain amino acids were also shown to restore the hybridoma growth rate, although only glycine betaine was found to restore specific productivity at high carbon dioxide levels [57]. In a separate study, antibody productivity was observed to increase by 50% with increased osmolality, which was attributed to improved antibody processing and assembly in the secretory pathway [58]. In another hybridoma example, an IgG3 was observed to have increased galactosylation at higher pH (pH 7.4 versus 7.2 and 6.9) and an increased ratio of *N*-acetylneuraminic acid to *N*-glycolylneuraminic acid [59].

A series of four antibody-producing CHO lines, differing in gene copy number, were also evaluated under hyperosmotic conditions. Antibody productivity was observed to increase most significantly in the lines with the lowest gene dosages (and corresponding mRNA levels) [60]. A proteomics approach was used to investigate the mechanism underlying the beneficial aspects of hyperosmolality on antibody specific productivity in CHO culture. The study identified an upregulation of certain glycolytic enzymes that could lead to increased metabolic energy in these cultures [61].

The effects of temperature have also been evaluated in recent studies. One recent analysis of antibody production in a CHO cell line showed no change in specific productivity at reduced temperature, which contrasts with other reports including a study using the same CHO host and a cytomegalovirus promoter with a different protein [62,63]. In another system, specific Fab production by a CHO line was seen to increase at reduced temperatures [64]. These results demonstrate that the effects of temperature might be cell-line specific. Given that the optimal temperature for growth and productivity can differ for a given cell line, a modeling approach was recently reported to aid identification of the optimal profile for a given process [65].

Complex raw materials such as hydrolysates are still commonly used in cell-culture processes, although the mechanisms for the benefits of these additives are not well understood and may vary between cell lines. A recent study in which certain di- to pentapeptides were added to the medium showed increased monoclonal antibody production in hybridoma cultures using specific peptides, supporting at least one possible type of beneficial component in the hydrolysates [66]. In another recent study, a hollow-fiber microbioreactor was used to distinguish between the effects of fresh medium on hybridoma specific productivity and conditioned medium in increasing cell density [67].

### Conclusions

As the clinical applications and needs for recombinant antibodies and antibody fragments have increased in recent years, the need for improvements in expression technologies to support these demands has correspondingly increased. Much recent work has led to significant improvements in the development of multiple expression platforms across the range of microbial, fungal, plant and mammalian systems. Improvements in the microbial production of antibodies and fragments have resulted from host-cell engineering to give increased productivity. There is also a trend towards producing antibodies or fragments with increased circulating half-life. This can be done either post-translationally, by adding PEG moieties, or during translation by adding an albumin-binding peptide or by expressing full-length IgG. There is a growing interest with both fungal and plant systems to address the issues surrounding non-mammalian glycosylation, either through glycosylation engineering or through the mutagenesis of glycosylation sites. For the case of mammalian systems, a growing trend has been towards manipulation of specific cellular pathways to improve performance, both regarding protein titers and antibody characteristics. The development of these approaches has also led to an increased understanding of the fundamental cellular phenomena controlling cell growth, death and productivity in these systems.

## Acknowledgements

The authors would like to thank Brad Snedecor and Bill Bennett for their critical review of the manuscript and suggestions.

## References and recommended reading

Papers of particular interest, published within the annual period of review, have been highlighted as:

- of special interest
- of outstanding interest

1. Humphreys DP, Glover DJ: Therapeutic antibody production technologies: molecules, applications, expression and purification. *Curr Opin Drug Discov Dev* 2001, 4:172-185.
2. Humphreys DP: Production of antibodies and antibody fragments in *Escherichia coli* and a comparison of their functions, uses, modifications. *Curr Opin Drug Discov Dev* 2003, 6:188-196.
- A detailed overview of the different types of antibody fragments and their production in *E. coli*.
3. Hood EE, Woodard SL, Horn ME: Monoclonal antibody manufacturing in transgenic plants – myths and realities. *Curr Opin Biotechnol* 2002, 13:630-635.
4. Roque ACA, Lowe CR, Taipa MA: Antibodies and genetically engineered related molecules: production and purification. *Biotechnol Prog* 2004, 20:639-654.
5. Chen C, Snedecor B, Nishihara JC, Joly JC, McFarland N, Andersen DC, Battersby JE, Champion KM: High-level accumulation of a recombinant antibody fragment in the periplasm of *Escherichia coli* requires a triple-mutant (*degP* *prc* *spv*) host strain. *Biotechnol Bioeng* 2004, 85:463-474.
6. Humphreys DP, Carrington B, Bowering LC, Ganesh R, Sehdev M, Smith BJ, King LM, Reeks DG, Lawson A, Popplewell AG: A plasmid system for optimization of Fab' production in *Escherichia coli*: Importance of balance of heavy chain and light chain synthesis. *Protein Expr Pur* 2002, 26:309-320.
7. Ramm K, Plückthun A: The periplasmic *Escherichia coli* peptidylprolyl *cis*, *trans*-isomerase FkpA. *J Biol Chem* 2000, 275:17106-17113.
8. Humphreys DP, Weir N, Lawson A, Mountain A, Lund PA: Co-expression of human protein disulphide isomerase (PDI) can increase the yield of an antibody Fab' fragment expressed in *Escherichia coli*. *FEBS Lett* 1996, 380:194-197.
9. Chapman AP, Antoniw P, Spitali M, West S, Stephens S, King DJ: Therapeutic antibody fragments with prolonged *in vivo* half-lives. *Nat Biotechnol* 1999, 17:780-783.
10. Leong SR, DeForge L, Presta L, Gonzalez T, Fan A, Reichert M, Chuntharapai A, Kim KJ, Tumas DB, Lee WP et al.: Adapting pharmacokinetic properties of a humanized anti-interleukin-8 antibody for therapeutic applications using site-specific pegylation. *Cytokine* 2001, 16:106-119.
11. Chapman AP: PEGylated antibodies and antibody fragments for improved therapy: a review. *Adv Drug Deliv Rev* 2002, 54:531-545.
12. Dennis MS, Zhang M, Meng G, Kadkhodayan M, Kirchhofer D, Combs D, Damico LA: Albumin binding as a general strategy for improving the pharmacokinetics of proteins. *J Biol Chem* 2002, 277:35035-35043.
- This report demonstrates the use of protein engineering to develop a novel peptide sequence that influences pharmacokinetics.
13. Simmons LC, Reilly D, Klimowski L, Raju TS, Meng G, Sims O, Hong K, Shields RL, Damico LA, Rancatore P, Yancura DG: Expression of full-length immunoglobulins in *Escherichia coli*: rapid and efficient production of aglycosylated antibodies. *J Immunol Methods* 2002, 263:133-147.
- The first report of the production of functional full-length IgGs in *E. coli*.
14. Sotiriadis A, Keshavarz T, Keshavarz-Moore E: Factors affecting the production of a single-chain antibody fragment by *Aspergillus awamori* in a stirred tank reactor. *Biotechnol Prog* 2001, 17:618-623.
15. Ward M, Lin C, Victoria DC, Fox BP, Fox JA, Wong DL, Meerman HJ, Pucci JP, Fong RB, Heng MH et al.: Characterization of humanized antibodies secreted by *Aspergillus niger*. *Appl Environ Microbiol* 2004, 70:2567-2576.
- An interesting study on using *A. niger* for the production of antibodies and fragments.
16. Hamilton SR, Bobrowicz P, Bobrowicz B, Davidson RC, Li H, Mitchell T, Nett JH, Rausch S, Stadheim TA, Wischniewski H et al.: Production of complex human glycoproteins in yeast. *Science* 2003, 301:1244-1246.
- This approach represents a powerful technique for host cell engineering to alter glycosylation of recombinant proteins.
17. Freyre FM, Vazquez JE, Ayala M, Canaan-Haden L, Bell H, Rodriguez I, Gonzalez A, Cintado A, Gavilondo JV: Very high expression of an anti-carcinoembryonic antigen single chain Fv antibody fragment in the yeast *Pichia pastoris*. *J Biotechnol* 2000, 78:157-163.
18. Cunha AE, Clemente JJ, Gomes R, Pinto F, Thomas M, Miranda S, Pinto R, Moosmayer D, Donner P, Carrondo MJT: Methanol induction optimization for scFv antibody fragment production in *Pichia Pastoris*. *Biotechnol Bioeng* 2004, 86:458-467.
19. Bakker H, Bardor M, Molthoff JW, Gomord V, Elbers J, Stevens LH, Jordi W, Lommen A, Faye L, Lerouge P, Bosch D: Galactose-extended glycans of antibodies produced by transgenic plants. *Proc Natl Acad Sci USA* 2001, 98:2899-2904.
20. Xie L, Pilbrough W, Metallo C, Zhong T, Pikus L, Leung J, Aunins J, Zhou W: Serum-free suspension cultivation of PER.C6 cells and recombinant adenovirus production under different pH conditions. *Biotechnol Bioeng* 2002, 80:569-579.
21. Jones D, Kroos N, Anema R, van Montfort B, Voors A, van der Kraats S, van der Helm E, Smits S, Schouten J, Brouwer K et al.: High-level expression of recombinant IgG in the human cell line PER.C6. *Biotechnol Prog* 2003, 19:163-168.
22. Bianchi AA, McGrew JT: High-level expression of full-length antibodies using trans-complementing expression vectors. *Biotechnol Bioeng* 2003, 84:439-444.
- An interesting approach to ensure co-amplification of heavy and light chains.
23. Aldrich TL, Vajda A, Morris AE: EASE vectors for rapid stable expression of recombinant antibodies. *Biotechnol Prog* 2003, 19:1433-1438.
24. Andersen DC, Krummen L: Recombinant protein expression for therapeutic applications. *Curr Opin Biotechnol* 2002, 13:117-123.
25. Fussenegger M, Bailey JE, Hauser H, Mueller PP: Genetic optimization of recombinant glycoprotein production by mammalian cells. *Trends Biotechnol* 1999, 17:35-42.
26. Barnes LM, Bentley CM, Dickson AJ: Stability of protein production from recombinant mammalian cells. *Biotechnol Bioeng* 2003, 81:631-639.
27. Kim NS, Byun TH, Lee GM: Key determinants in the occurrence of clonal variation in humanized antibody expression of CHO cells during dihydrofolate reductase mediated gene amplification. *Biotechnol Prog* 2001, 17:69-75.
28. Brezinsky SC, Chiang GG, Szilvasi A, Mohan S, Shapiro RI, Maclean A, Sisk W, Thill G: A simple method for enriching populations of transfected CHO cells for cells of higher specific productivity. *J Immunol Methods* 2003, 277:141-155.
29. Bailey CG, Tait AS, Sunstrom N-A: High-throughput clonal selection of recombinant CHO cells using a dominant selectable and amplifiable metallothionein-GFP fusion protein. *Biotechnol Bioeng* 2002, 80:670-676.
30. Borth N, Zeyda M, Kättinger H: Efficient selection of high-producing subclones during gene amplification of recombinant Chinese hamster ovary cells by flow cytometry and cell sorting. *Biotechnol Bioeng* 2000-2001, 71:256-273.
31. Meents H, Enenkel B, Werner RG, Fussenegger M: p27Kip1-mediated controlled proliferation technology increases

- constitutive sICAM production in CHO-DUKX adapted for growth in suspension and serum-free media. *Biotechnol Bioeng* 2002, 79:819-827.
32. Carvahal AV, Marcelino I, Carrondo MJT: Metabolic changes during cell growth inhibition by p27 overexpression. *Appl Microbiol Biotechnol* 2003, 63:164-173.
  33. Bi J-X, Shuttleworth J, Al-Rubeai M: Uncoupling of cell growth and proliferation results in enhancement of productivity in p21cip1-arrested CHO cells. *Biotechnol Bioeng* 2004, 85:741-749.
  34. Altamirano C, Calro JJ, Godia F: Decoupling cell growth and product formation in Chinese hamster ovary cells through metabolic control. *Biotechnol Bioeng* 2001, 76:351-360.
  35. Carvahal AV, Sa Santos S, Calado J, Haury M, Carrondo MJT: Cell growth arrest by nucleotides, nucleosides and bases as a tool for improved production or recombinant proteins. *Biotechnol Prog* 2003, 19:89-93.
  36. Yuk IHY, Wildt S, Jolicœur M, Wang DIC, Stephanopoulos G: A GFP-based screen for growth-arrested recombinant protein-producing cells. *Biotechnol Bioeng* 2002, 79:74-82.
  37. Mastrangelo AJ, Hardwick JM, Zou S, Betenbaugh MJ: Part 2. Over-expression of bcl-2 family members enhances survival of mammalian cells in response to various culture insults. *Biotechnol Bioeng* 2000, 67:555-564.
  38. Figueroa B Jr, Chen S, Oyler GA, Hardwick JM, Betenbaugh MJ: Aven and bcl-x<sub>L</sub> enhance protection against apoptosis for mammalian cells exposed to various culture conditions. *Biotechnol Bioeng* 2004, 85:589-600.
  39. Sauerwald TM, Oyler GA, Betenbaugh MJ: Study of caspase inhibitors for limiting cell death in mammalian cell culture. *Biotechnol Bioeng* 2003, 81:329-340.
  40. Kim NS, Lee GM: Inhibition of sodium butyrate-induced apoptosis in recombinant Chinese hamster ovary cells by constitutively expressing antisense RNA of caspase-3. *Biotechnol Bioeng* 2002, 78:217-228.
  41. Lasunskaja EB, Fridlanskaia II, Darieva ZA, da Silva MSR, Kanashiro MM, Margulis BA: Transfection of NS0 myeloma fusion partner cells with hsp70 gene results in higher hybridoma yield by improving cellular resistance to apoptosis. *Biotechnol Bioeng* 2003, 81:496-504.
  42. Lee SK, Lee GM: Development of apoptosis-resistance dihydrofolate reductase-deficient Chinese hamster ovary cell line. *Biotechnol Bioeng* 2003, 82:872-876.
  43. Meents H, Enekel B, Eppenberger HM, Werner RG, Fussenegger M: Impact of coexpression and coamplification of sICAM and antiapoptosis determinants bcl-2/bcl-x<sub>L</sub> on productivity, cell survival, and mitochondrial number in CHO-DG44 grown in suspension and serum-free media. *Biotechnol Bioeng* 2002, 80:706-718.
  44. Jung D, Cote S, Drouin M, Simard O, Lamieux R: Inducible expression of bcl-x<sub>L</sub> restricts apoptosis resistance to the antibody secretion phase in hybridoma cultures. *Biotechnol Bioeng* 2002, 79:180-187.
  45. Ibarra N, Watanabe S, Bi JX, Shuttleworth J, Al-Rubeai M: Modulation of cell cycle for enhancement of antibody productivity in perfusion culture of NS0 cells. *Biotechnol Prog* 2003, 19:224-228.
  - Combines growth control and anti-apoptosis engineering to enhance antibody productivity.
  46. Lambert N, Merten O-W: Effect of serum-free and serum-containing medium on cellular levels of ER-based proteins in various mouse hybridoma cell lines. *Biotechnol Bioeng* 1997, 54:165-180.
  47. Chung JY, Lim SW, Hong YJ, Hwang SO, Lee GM: Effect of doxycycline-regulated calnexin and calreticulin expression on specific thrombopoietin productivity of recombinant Chinese hamster ovary cells. *Biotechnol Bioeng* 2004, 88:539-548.
  48. Wright A, Morrison SL: Effect of glycosylation on antibody function: Implications for genetic engineering. *Trends Biotechnol* 1997, 15:26-32.
  49. Jefferis R: Glycosylation of human IgG antibodies: relevance to therapeutic applications. *Biopharm* 2001, 9:19-27.
  50. Shields RL, Lai J, Keck R, O'Connell LY, Hong K, Meng YG, Weikert SH, Presta LG: Lack of fucose on human IgG1 N-linked oligosaccharide improves binding to human Fc-γ RIII and antibody-dependent cellular toxicity. *J Biol Chem* 2002, 277:26733-26740.
  - Significant improvements in ADCC result from alteration of the oligosaccharides on Fc.
  51. Shinkawa T, Nakamura K, Yamane N, Shoji-Hosaka E, Kanda Y, Sakurada M, Uchida K, Anazawa H, Satoh M, Yamasaki M et al.: The absence of fucose but not the presence of galactose or bisecting N-acetylglucosamine of human IgG1 complex-type oligosaccharides shows the critical role of enhancing antibody-dependent cellular cytotoxicity. *J Biol Chem* 2003, 278:3466-3473.
  52. Presta LG, Shields RL, Namenuk AK, Hong K, Meng YG: Engineering therapeutic antibodies for improved function. *Biochem Soc Trans* 2002, 30:487-490.
  53. Hinton PR, Johlfs MG, Xiong JM, Hanestad K, Ong KC, Bullock C, Keller S, Tang MT, Tso JY, Vasquez M, Tsurushita N: Engineered human IgG antibodies with longer serum half-lives in primates. *J Biol Chem* 2004, 279:6213-6216.
  54. Osman JJ, Birch J, Varley J: The response of GS-NS0 myeloma cells to single and multiple pH perturbations. *Biotechnol Bioeng* 2003, 79:398-407.
  55. DeZengotita VM, Schmelzer AE, Miller WM: Characterization of hybridoma cell responses to elevated pCO<sub>2</sub> and osmolality: Intracellular pH, cell size, apoptosis, and metabolism. *Biotechnol Bioeng* 2002, 77:369-380.
  56. Schmelzer AE, Miller WM: Hyperosmotic stress and elevated pCO<sub>2</sub> alter monoclonal antibody charge distribution and monosaccharide content. *Biotechnol Prog* 2002, 18:346-353.
  57. DeZengotita VM, Abston LR, Schmelzer AE, Shaw S, Miller WM: Selected amino acids protect hybridoma and CHO cells from elevated carbon dioxide and osmolality. *Biotechnol Bioeng* 2002, 78:741-752.
  58. Sun Z, Zhou R, Liang S, McNeeley KM, Sharfstein ST: Hyperosmotic stress in murine hybridoma cells: effects on antibody transcription, translation, posttranslational processing and the cell cycle. *Biotechnol Prog* 2004, 20:576-589.
  59. Muthing J, Kemminer SE, Conradt HS, Sagl D, Nimtz M, Karst U, Pater-Katafinc J: Effects of buffering conditions and culture pH on production rates and glycosylation of clinical phase I anti-melanoma mouse IgG3 monoclonal antibody R24. *Biotechnol Bioeng* 2003, 83:321-334.
  60. Ryu JS, Lee MS, Lee GM: Effects of cloned gene dosage on the response of recombinant CHO cells to hyperosmotic pressure in regard to cell growth and antibody production. *Biotechnol Prog* 2001, 17:993-999.
  61. Lee MS, Kim KW, Kim YH, Lee GM: Proteome analysis of antibody-expressing CHO cells in response to hyperosmotic pressure. *Biotechnol Prog* 2003, 19:1734-1741.
  62. Yoon SK, Kim SH, Lee GM: Effect of low temperature on specific productivity and transcription level of anti-4-BB antibody in recombinant Chinese hamster ovary cells. *Biotechnol Prog* 2003, 19:1383-1386.
  63. Yoon SK, Song JY, Lee GM: Effect of low temperature on specific productivity, transcription level, and heterogeneity of erythropoietin in Chinese hamster ovary cells. *Biotechnol Bioeng* 2003, 82:289-298.
  64. Schatz SM, Kerschbaumer RJ, Gerstenbauer G, Kral M, Dörner F, Scheiflinger F: Higher expression of Fab antibody fragments in a CHO cell line at reduced temperature. *Biotechnol Bioeng* 2003, 84:433-438.
  65. Fox SR, Patel UA, Yap MGS, Wang DIC: Maximizing interferon-γ production by Chinese hamster ovary cells through temperature shift optimization: experimental and modeling. *Biotechnol Bioeng* 2004, 85:177-184.

66. Franek F, Eckschlager T, Katinger H: Enhancement of monoclonal antibody production by lysine-containing peptides. *Biotechnol Prog* 2003, 19:169-174.

67. Gramer MJ, Britton TL: Antibody production by a hybridoma cell line at high cell density is limited by two independent mechanisms. *Biotechnol Bioeng* 2002, 79:277-283.

Nature 341, 544 - 546 (12 October 1989)

Binding activities of a repertoire of single immunoglobulin variable domains secreted from *Escherichia coli*

E. Sally Ward, Detlef Güssow, Andrew D. Griffiths, Peter T. Jones & Greg Winter\*

In antibodies, a heavy and a light chain variable domain, VH and VL, respectively, pack together and the hypervariable loops on each domain contribute to binding antigen<sup>1-4</sup>. We find, however, that isolated VH domains with good antigen-binding affinities can also be prepared. Using the polymerase chain reaction<sup>5</sup>, diverse libraries of VH genes were cloned from the spleen genomic DNA of mice immunized with either lysozyme or keyhole-limpet haemocyanin. From these libraries, VH domains were expressed and secreted from *Escherichia coli*. Binding activities were detected against both antigens, and two VH domains were characterized with affinities for lysozyme in the 20 nM range. Isolated variable domains may offer an alternative to monoclonal antibodies and serve as the key to building high-affinity human antibodies. We suggest the name 'single domain antibodies (dAbs)' for these antigen binding demands.

## Antigen Specificity and High Affinity Binding Provided by One Single Loop of a Camel Single-domain Antibody\*

Received for publication, March 8, 2001, and in revised form, May 3, 2001  
Published, JBC Papers in Press, May 7, 2001, DOI 10.1074/jbc.M102107200

Aline Desmyter†, Klaas Decanniere, Serge Muyldermans, and Lode Wyns

From the Department Ultrastructure, Vlaams Interuniversitair Instituut voor Biotechnologie, Vrije Universiteit Brussel, Paardenstraat 65, B-1640 Sint Genesius Rode, Belgium

Detailed knowledge on antibody-antigen recognition is scarce given the unlimited antibody specificities of which only few have been investigated at an atomic level. We report the crystal structures of an antibody fragment derived from a camel heavy chain antibody against carbonic anhydrase, free and in complex with antigen. Surprisingly, this single-domain antibody interacts with nanomolar affinity with the antigen through its third hypervariable loop (19 amino acids long), providing a flat interacting surface of 620 Å<sup>2</sup>. For the first time, a single-domain antibody is observed with its first hypervariable loop adopting a type-I canonical structure. The second hypervariable loop, of unique size due to a somatic mutation, reveals a regular  $\beta$ -turn. The third hypervariable loop covers the remaining hypervariable loops and the side of the domain that normally interacts with the variable domain of the light chain. Specific amino acid substitutions and reoriented side chains reshape this side of the domain and increase its hydrophilicity. Of interest is the substitution of the conserved Trp-103 by Arg because it opens new perspectives to 'humanize' a camel variable domain of heavy chain of heavy chain antibody (VHH) or to 'camelize' a human or a mouse variable domain of heavy chain of conventional antibody (VH).

Conventional antibody IgG molecules consist of two light chains folded in two domains and two heavy chains folded in four domains (1). Surprisingly, the serum of *Camelidae* contains in addition a large proportion (~50%) of functional antibodies devoid of light chains and heavy chains possessing only three domains since the equivalent of the first constant domain is missing (2). The two C-terminal domains of the heavy chain homodimers within camelids and conventional IgG molecules share large sequence identities and are responsible for the effector functions. Also, the N-terminal variable domain of the heavy chain antibodies (referred to as VHH)<sup>1</sup> (3) has an overall

sequence and structure that is homologous to the variable domain (VH) of the heavy chain of a classical human antibody (4–8). Important amino acid differences occur between the VH and VHH in their framework 2 region. This region is hydrophilic in VHHs rendering the domain soluble in aqueous solution, whereas the region is hydrophobic in the VH, and its amino acids associate with the VL. The VHH domain represents the smallest naturally occurring, intact antigen-binding site (9), comprising only one single immunoglobulin domain with three antigen-binding loops (or complementarity determining regions, CDRs). Heavy chain antibodies with high specificity and affinity can be generated against a wide variety of antigens (10). Their VHHs are readily cloned (11, 12) and expressed in bacteria and yeast (13) and are extremely stable (14).

In human and mouse, the first two antigen-binding loops of a VH domain, CDR1 and CDR2, can be assigned to a limited number of possible conformations referred to as canonical structures (15–18). The conformation of these loops depends both on their length and on the presence of specific residues at key positions. In contrast, the x-ray structure analysis of four VHH domains showed that their CDR1 and CDR2 deviate significantly from the canonical loop structures observed in human or mouse VHs (19).

The third antigen-binding loop (CDR3) of the VHH fragments is often constrained by an interloop disulfide bond and is, on average, longer than a human or mouse VH-CDR3 loop (4). This allows for a potentially larger antigen-binding surface (20).

About half of the dromedary single-domain binders to enzymes are potent inhibitors (12). This can be explained by their long CDR3 loop inserting into the active site cleft on the enzyme surface, as illustrated by the lysozyme binder cAb-Lys3. In this case, the N-terminal part of the 24-amino acid-long CDR3 loop protrudes from the remaining antigen-binding surface, penetrates deeply into the active site of the enzyme (6), and mimics the lysozyme natural substrate (21). However, several non-inhibiting antibody fragments with a long CDR3 loop were also isolated (12), and these fragments are not expected to interact with the active site of their enzymes. Therefore, it was hypothesized that these non-inhibiting VHH molecules would interact with other clefts present on the protein surface.

Here, we present the crystal structures of a camel VHH fragment, cAb-CA05, both as free antibody and in complex with its antigen. This specific non-inhibiting enzyme binder recognizes the bovine erythrocyte carbonic anhydrase with an affinity of 72 nM ( $K_d$ ), which is in the same range as other VHHs or

\* This work was supported by Fonds voor Wetenschappelijk onderzoek, European Space Agency, and Prodex program for funding (12988/98/NL/VJ(IC)) and the Research & Technology Development Biotechnology program of the 4<sup>th</sup> EC framework (BIO4-98-0048). Travel to and accommodation in Hamburg was supported by the European Union TMR/LSF Grant ERBFMG3CT 980134.

The atomic coordinates and structure factors (code 1F3X, 1G6V) have been deposited in the Protein Data Bank, Research Collaboratory for Structural Bioinformatics, Rutgers University, New Brunswick, NJ (<http://www.rcsb.org/>).

† To whom correspondence should be addressed. Tel.: 32-0-2-35-90-268; Fax.: 32-0-2-35-90-289; E-mail: aldesmtr@vub.ac.be.

<sup>1</sup> The abbreviations used are: VHH, variable domain of heavy chain of heavy chain antibody; VH, variable domain of heavy chain of conventional antibody; VL, variable domain of light chain; CDR, complementarity determining region; cAb, camel single-domain antibody fragment; rmsd, root-mean-square deviations; hcg, human chorionic gonadotropin; H1 and H2, structural loop around, respectively, the first and second antigen-binding region of a VH.

single chain variable fragment (11, 12). Surprisingly, the structural data reveal for the first time an antibody using only one single loop, its CDR3, to interact directly with the antigen.

#### EXPERIMENTAL PROCEDURES

**Crystallization and Data Collection**—The cAb-CA05 was extracted from *Escherichia coli* periplasm and purified by chromatography on Ni-NTA (Qiagen) and Superdex 75 (Amersham Pharmacia Biotech) and gel filtration (12). The cAb-CA05-carbonic anhydrase complex was prepared by mixing cAb-CA05 in phosphate buffered saline with bovine erythrocyte carbonic anhydrase (Sigma) in a molar ratio of 1.2: 1 and applied on Superdex 75 (Amersham Pharmacia Biotech). Crystals from the antigen-free cAb-CA05 (1.7 mg/ml) and from the complex cAb-CA05-carbonic anhydrase (3.5 mg/ml) were grown in 25% (w/v) PEG8000 (Hampton), 0.1 M sodium citrate, pH 5.6, using the hanging drop vapor diffusion method.

A data set to 2.1 Å for cAb-CA05 was collected using a Rigaku RU-H2R rotating anode generator (Kobe, Japan) and a MarResearch image plate (MarResearch, Hamburg, Germany). Data for the antigen-antibody crystal were collected on beam line BW7A at EMBL-Hamburg using a MarResearch image plate. Primary data processing was done with DENZO (22), scaling was done with SCALA, and further processing was done with the CCP4 program suite (23).

**Structure Determination and Refinement**—The structure of the free antigen was solved by molecular replacement as implemented in AMORE (24), using the VHH cAb-RN05 (Protein Data Bank entry code 1B2Q) as a search model. The structure was refined with X-PLOR (25) and REFMAC (26). The CDR loops were deleted from the search model and rebuilt from scratch. Possible water positions were identified with ARP (27) and checked manually. Model and structure factors are deposited in the Protein Data Bank, entry 1F2X.

The antigen-antibody complex structure was solved by molecular replacement with the antigen-free cAb-CA05 structure and human carbonic anhydrase structure (1CA2) as search models. For refinement, we used the CNS program (28), and included a simulated-annealing step to reduce possible model bias. As the high resolution limit of the data set is 3.5 Å, a grouped B factor refinement scheme was used (only one B factor for main chain atoms and one B factor for side chain atoms/residue). Model and structure factors are accessible through the Protein Data Bank, entry 1G6V.

Superposition of structures or structure fragments and calculation of rmsd were done with LSQKAB (23). Inter-residue and inter-atom distances were calculated with CONTACT (23), and accessible surface areas were calculated with NACCESS (29). Figures were produced with MOLSCRIPT 2.1 (30) and rendered with RASTER3D (31).

#### RESULTS

**cAb-CA05 Sequence and General Structure**—cAb-CA05 is a VHH antibody fragment of 135 residues ( $M_r$  15,000) that binds specifically to bovine erythrocyte carbonic anhydrase ( $K_d = 72$  nM) but does not inhibit the enzymatic activity of the antigen. It was selected by panning from a VHH library of an immunized dromedary (12). The cAb-CA05 shares a high sequence identity with other VHHs or human VHs of family III (Fig. 1). Nevertheless, the VHH characteristic amino acids in framework 2 (Phe-37, Glu-44, Arg-45, and Gly-47) (4, 20) are all present (Kabat amino acid numbering (32)). In addition, residue Trp-103, constitutively conserved in all VHs and interacting with the VL, is substituted by Arg in cAb-CA05. Like most other VHHs from camelids, the cAb-CA05 contains a long CDR3 (19 amino acids) with a cysteine at position 100c expected to form a disulfide bond with Cys-33 located in the CDR1. The CDR2 of cAb-CA05 is unusually short as it contains 15 amino acids instead of a standard length of 16, 17, or 19 amino acids (32).

The cAb-CA05 was crystallized both as free antibody and in complex with its antigen. Antigen-free cAb-CA05 crystallizes in space group P 2<sub>1</sub> with cell dimensions of  $a = 29.98$  Å,  $b = 43.86$  Å,  $c = 87.95$  Å,  $\beta = 93.23^\circ$  and two VHH molecules in the asymmetric unit. The antigen-antibody complexes crystallize in space group P 4<sub>1</sub>2<sub>1</sub>2 with cell dimensions of  $a = 83.86$  Å and  $c = 224.05$  Å and one antigen-antibody complex in the asymmetric unit.

cAb-CA05	<-----FRAMEWORK 1----->	<---H1/CDR1--->
cAb-Lys3	QVQLVSGGGSVQAGGSLRLSCAAS	GYT---VSTYCMG
cAb-RN05	DVQLQASGGGVSQAGGSLRLSCAAS	GYT---IGPYCMG
llama hcg	QVQLVESGGGLVQAGGSLRLSCAAS	GYA---YTYIYMG
llama RR6	QVQLQESGGGLVQAGGSLRLSCAAS	GRT---GSTYDMG
Pot VH	EVNLLSGGNLVQPCCSLRLSCAAS	GFT---FNIFVYS
	1 10 20 25 30 35	
	<---FRAMEWORK 2--->	<---FRAMEWORK 3--->
	WFRQAPGKEREQVA TIL--GGSTYYGDSVKG	RFTISQDNAKNTVYLQMN
	WFRQAPGKEREQVA AINMGGGITYYAOSVKG	RFTISQDNAKNTVYLLMN
	WFRQAPGKEREQVA AMDSGGGGLYADSVKG	RFTISRDKGKNTVYLQMD
	WFRQAPGKEREQVA AINWDSARTYASSVKG	RFTISRDNAKKTVYLQMN
	WFRQAPGKEREQVA AIRWSGKETWYKDSVKG	RFTISRDNAKKTVYLQMN
	WFRQAPGKEREQVA GVFGSGGNTDYADAVKG	RFTITRDNKNTVYLQMN
	40 50 52 60 65 70 80 82a	
	<---FRAMEWORK 3--->	<---FRAMEWORK 4--->
	SLKPEDTAIYYCAG STVASTGWCSSLRLRPDY	HY RGQGTQVTVSS
	SLKPEDTAIYYCAA DSTIYASYYECGHLSTGGYVDS	WGQGTQVTVSS
	SLKPEDTAIYYCAA GGYELDRDTY	CG WGQGTQVTVSS
	SLKPEDTAVYTCGA GEGGTH	DS WGQGTQVTVSS
	SLKPEDTAVYCAA RPVRVDDISLPVGF	DY WGQGTQVTVSS
	SLRAEDTAIYYCAK HRVSYVLTGF	DS WGQGTQVTVSS
	bc 90 94 100 abcdefghijklmno 103 110	

Fig. 1. Amino acid sequence alignment of VHHs and a human VH of known structure. The sequences of cAb-CA05 (this study), cAb-Lys3 (6), cAb-RN05 (5), llama VHH hcg (7), RR6 (8), and human Pot VH (50) are shown. The frameworks, the CDRs and the amino acid numbering (bottom line) are as defined by Kabat *et al.* (32). The VHH-specific amino acids of the framework 2 region are in bold and an asterisk indicates their location.

TABLE I  
Crystallographic data and refinement statistics for antigen-free and antigen-complexed cAb-CA05

Data statistics (highest shell)	Antigen-free	Antigen-complexed
Resolution limits (Å)	31.0–2.1 (2.21–2.1)	26.5–3.5 (3.69–3.5)
R factor (%)	10.3 (22.7)	15.9 (34.5)
Completeness	99.8 (99.8)	99 (99)
I/ $\sigma$	4.9 (2.7)	4.4 (2.1)
Multiplicity	5.8 (5.3)	5.6 (5.8)
Refinement statistics		
# of reflections	12786	10533
# of reflections free	686	603
R (%)	19.0	21.0
Rfree (%)	27.0	27.6
Geometry		
Rmsd bond lengths (Å)	0.009 (refmac)	0.008 (cns)
Rmsd bond angles (°)	0.027 (refmac)	1.360 (cns)
Rmsd planarity (Å)	0.026	/
ESU <sup>a</sup> Rfree (Å)	0.23	/
ESU ML <sup>b</sup> residual (Å)	0.15	/

<sup>a</sup> ESU, estimated standard uncertainty.

<sup>b</sup> ESU ML, estimated standard uncertainty maximum likelihood.

The structure of the antigen-free cAb-CA05 was refined to 2.1 Å resolution (Table I). It adopts the standard fold of an immunoglobulin variable domain with nine conserved antiparallel  $\beta$ -strands (Fig. 2) and three hypervariable regions clustering at one end of the domain (1, 33, 34). The Cys-22 and Cys-92 are oxidized into an intradomain disulfide bond, conserved in all immunoglobulin domains. Its general structure superimposes very well with a human VH reference structure (1igm) and with all available VHH structures of camel (1mel, 1b2q) and llama (1hcv, 1qdo). Root-mean-square deviations for the main chain atoms of the framework residues (residues 2–24, 32–52, 55–72, 77–92, and 103–112) ranged between 0.58 and 0.88 Å.

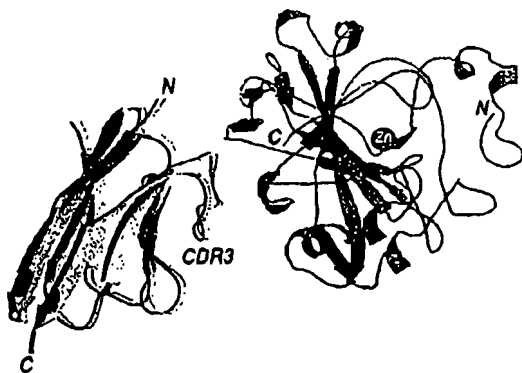


FIG. 2. Superposition of antigen-free cAb-CA05 and carbonic anhydrase complexed cAb-CA05. The structure of one of the molecules of cAb-CA05 as it occurs in the antigen-free crystal is superimposed on the cAb-CA05 structure of the antigen-complexed crystal. The carbonic anhydrase is on the right end of the figure with the Zn ion of the active site indicated. To enhance the visualization of the two VHH molecules, we translated the free cAb-CA05 by 0.8 Å to the left relative to the cAb-CA05-antigen complex. The N- and C-ends and the CDR3 location of the molecules are given for reference.

Structural adaptations, however, are expected to occur in the side of the domain that corresponds to the VL-interacting side of a VH domain. This area is hydrophobic in all VHs by the presence of Val-37, Leu-45, Trp-47, and Trp-103 side chains, conserved in sequence and structural position (Fig. 3A) (35). The L45R and W47G substitutions and the Trp-103 rotated over its C $\beta$ -C $\gamma$  bond in cAb-Lys3 (Fig. 3C) make this VHH region more hydrophilic. The V37F mutation fills a hydrophobic pocket created by the side chains of the Trp-103, Tyr-91, and the CDR3, where the conserved Tyr (three amino acids upstream of Trp-103) plays a central role (6). The W103R substitution found here in cAb-CA05 renders this 'former VL side' of the VHH even more hydrophilic. It also allows a shift of the Phe-37 side chain toward the Tyr-91 and Arg-103 (Fig. 3D). As a result, the backbone of the long CDR3 approaches the former VL-side even more closely (Fig. 4D). All these modifications occur in the absence of distortions of the framework structure. In contrast, the partial camelization of a human VH in this area by L45R and W47I substitutions makes the isolated domain more soluble but induces backbone deformations at positions 37–38 and 45–47 (36). In addition, the side chain of Trp-103 takes a completely new position (Fig. 3B).

**cAb-CA05 Hypervariable Regions**—The conformation of the H1 loop (residues 26–32, the solvent-exposed loop around the CDR1) of cAb-CA05 fits with the canonical structure type-1, a conformation observed in all VH structures containing a 7-amino acid H1 loop (15, 16). This canonical loop structure is shaped by a sharp turn at Gly-26, clustering of the hydrophobic side chains of Ala-24, Phe-27, Phe-29, and Met-34 (Fig. 4A), and the hydrophobic part of the Arg-94 side chain (C $\delta$ -C $\epsilon$  of Lys-94 in Pot VH) (16). The sequence composition of the cAb-CA05 H1 loop harbors the key elements for a type-1 structure except for the R94G and conservative F27Y and F29V substitutions (Fig. 1). These substitutions lead to a slightly different organization of the side chains forming the hydrophobic core of the loop but do not influence the main chain conformation of the loop (Fig. 4A). In contrast, all previously solved camel or llama VHH structures had their H1 loop folded into completely different main chain architectures.

Residues 52–56 form a hairpin loop (denoted H2) that constitutes the antigen-binding region of the second hypervariable region (15, 16). Canonical structures of the H2 loop are described for loops with sizes of five, six, or eight amino acids. We

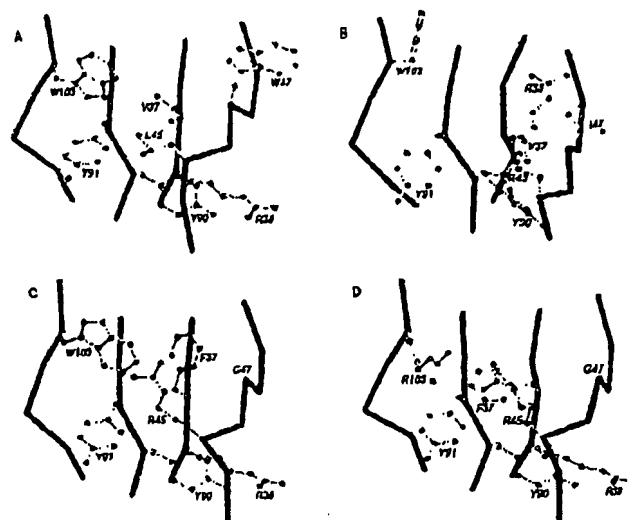


FIG. 3. Structural organization of the VL-facing side of a VH and its corresponding side in VHHs and a partial camelized human VH. A, VL eye-view of a human VH (1igm, Ref. 50). B, the partial camelized human VH (1vhp, Ref. 36). C, the corresponding side of a VHH, cAb-Lys3 (1mel, Ref. 6) and D, cAb-CA05 (this study). The side chain of residues that take a different conformation among VH and VHH are shown in ball-and-stick and are denoted by their single letter code. The side chains of Arg-38, Tyr-90, and Tyr-91 having similar orientations in VH and VHHs are shown for reference.

previously showed that VHH H2 loops of six amino acids adopt conformations not yet observed in VH structures (19). Here, we are facing an H2 loop with only four amino acids (Fig. 1) that adopts a regular  $\beta$ -hairpin structure (Fig. 4B) known as type II' (37). A comparison of four- and five-amino acid-long H2 loops indicates that the addition of a fifth amino acid introduces a bulge at position 55 and converts the loop to an H2 canonical structure type-1 (Fig. 4, B and C).

The CDR3 (residues 95–102) of a VHH is on average longer than that of a VH (17 versus 12 residues) (4), although a notable fraction of llama VHHs were found with 'short' CDR3 loops (20, 38). Another remarkable feature of the CDR3 of VHHs is the frequent presence of a cysteine forming a disulfide bond with a cysteine in the CDR1 (4, 6). In this respect, the cAb-CA05 with a 19-amino acid-long CDR3 loop and cysteines at positions 33 and 100c forming a disulfide bond is comparable with cAb-Lys3 (6) (Figs. 1 and 4D).

The cysteine at position 100c can be considered to divide the CDR3 region into an N-terminal and a C-terminal part. The C-terminal part of the CDR3 loop folds back onto the side of the VHH domain corresponding to the side of the VH interacting with VL (1) (see Table II for a list of contacting residues) (39). Large parts of the former VL-side are apparently shielded from the solvent by the C-end of the CDR3. A similar location and function has been observed for the C-terminal part of the cAb-Lys3 CDR3-loop (Fig. 4D) (6) for the entire, much shorter CDR3 loop of cAb-RN05 (5) and that of RR6 llama VHH (8).

The N-terminal part of the CDR3 of cAb-CA05 and cAb-Lys3 are in a different environment. In cAb-Lys3, it forms a protruding loop (Fig. 4D) inserting in the catalytic site of the lysozyme (21). In cAb-CA05, this part of the loop does not extend into the solvent but associates with the residues of the remaining hypervariable loops (Table II). Thus, the N-terminal and C-terminal half of the CDR3 of cAb-CA05 contact different parts of the domain. Furthermore, the entire (long) CDR3 of cAb-CA05 appears to be well fixed by these abundant contacts and by the covalent Cys33-Cys100c disulfide bond.



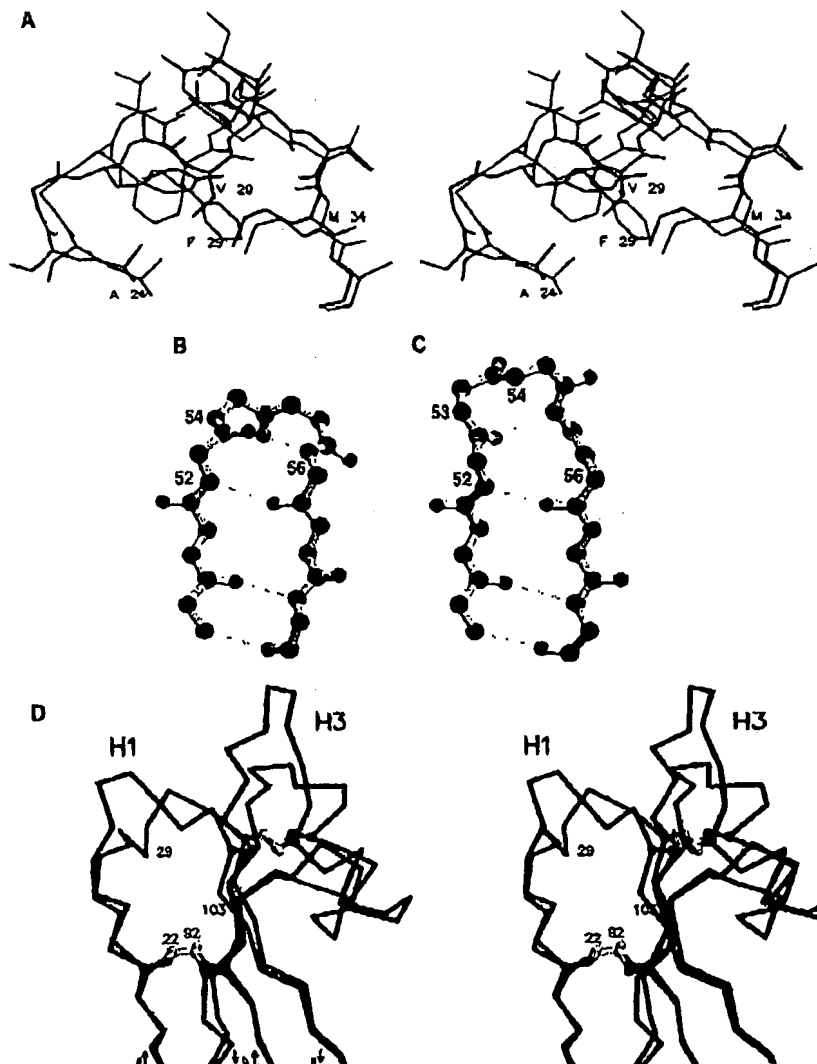


FIG. 4. Structure of the antigen-binding loops in cAb-CA05. A, stereo presentation of superposition of the H1 loop of the human Pot VH (1igm) adopting a type-1 canonical structure (brown) and the cAb-CA05 (blue) including the structure-determining side chains forming a hydrophobic core. B, the peptide backbone of the H2 loop of cAb-CA05 and C, of a canonical structure type-1 human VH (7fab) shown in ball-and-stick representation. The dashed lines indicate the inter-loop hydrogen bonds. D, stereo picture of the superposition of the H1 and H3 loops of cAb-Lys3 (1mel) (brown) and cAb-CA05 (blue and red, respectively). The interloop disulfide bond is shown as well as the conserved disulfide bond between the scaffold Cys-22 and Cys-82. The Kabat numbering of a few amino acids is given for reference.

**The Antigen-Antibody Complex**—In addition to the antigen-free cAb-CA05 crystal, crystals of the complex of cAb-CA05 with its antigen, carbonic anhydrase, were obtained and diffracted to 3.5 Å using synchrotron radiation. The structure was solved by molecular replacement (see "Experimental Procedures") and the data and refinement statistics for the antibody-antigen complex structure are shown in Table I.

Binding of the antibody has little influence on the overall structure of the carbonic anhydrase. The rmsd is 0.7 Å for the C $\alpha$  atoms between the bovine carbonic anhydrase molecule found here and the human carbonic anhydrase used as search model. Also, the structure of the cAb-CA05 antibody in the complex is the same as the uncomplexed structure (Fig. 2). The rmsd of the antibody in the complex with respect to the free antibody is 0.4 Å for all main chain atoms. Moreover, the hypervariable loops maintain their main chain conformation upon antigen binding; the H1 loop remains in the canonical structure type-1, the four-amino acid-long H2 loop keeps its conformation, and the structures of the CDR3 loops also resemble each other closely.

The epitope consists of two separate continuous segments within the carbonic anhydrase. A first stretch includes residues 46–52 and the second stretch involves residues 180–187 (Fig.

2, Table II). The first segment uses mainly main chain atoms (21 of 29 contacts), whereas the second part of the epitope involves mainly side chain atoms (50 of 58 contacts). The paratope comprises both, the N- and the C-terminal part of the CDR3 loop. In the N-terminal part of the CDR3, many main chain atoms participate in antigen binding; 32 of 60 contacts (i.e. antibody atoms within 4.0 Å of antigen atoms) involve an antibody main chain atom. In the C-terminal part of the CDR3, only antibody side chain atoms contact the antigen.

The antigen-interacting surface of cAb-CA05 is to a large extent planar (Fig. 5). A solvent-accessible surface area of 622 Å<sup>2</sup> becomes buried upon antigen complexation. Remarkably, the CDR3 region provides this surface entirely. The antigen makes no contacts with the CDR1 and CDR2 loops apart from Tyr-32, which is at 3.7 Å from the carbonic anhydrase molecule. This is the first antibody fragment that shows high affinity and high binding specificity using one CDR loop for direct interaction.

#### DISCUSSION

The crystal structures of cAb-CA05, both antigen-free and in complex with carbonic anhydrase, reveals the structural adaptations in the VHH that explain its solubility and antigen-

TABLE II  
CDR3 residues contacting the remaining VHH or antigen

Antibody residues contacting the CDR3 residues <sup>a</sup>	Interacting CDR3-residues <sup>a</sup>	Antigen residues contacting the CDR3 residues <sup>a</sup>
Tyr-27, Tyr-32, Cys-33	Ser-96	
Tyr-32	Thr-96	Leu-47, Ser-48, Val-49
Cys-33	Val-97	Val-49, Leu-189
Thr-31	Ala-98	Val-49, Ser-50, Tyr-51, Asp-52, Arg-182
		Asp-180, Arg-182
Leu-52	Ser-99	Asp-180
Leu-52, Tyr-58	Thr-100	Arg-182, Pro-186, Glu-187
	Gly-100a	
	Trp-100b	
Cys-33 <sup>d</sup> , Thr-50, Ile-51	Cys-100c <sup>d</sup>	
Tyr-58	Ser-100d	
	Arg-100e	Arg-182, Gly-183, Leu-185, Glu-187
Gly-47, Val-48, Tyr-59, Leu-60	Gly-100f	
	Arg-100g	Glu-187
Gly-35, Trp-36, Phe-37, Thr-60	Pro-100h	
Phe-37, Arg-45, Gly-47	Tyr-100i	
	Asp-100j	Glu-187
Cys-33, Met-34, Thr-50	Tyr-100k	
	His-101	Pro-46
Val-2, Leu-4	Tyr-102	
Leu-4, Phe-37	Arg-103	

<sup>a</sup> Residues of the antibody having atoms within 4.0 Å to CDR3; the residues in bold belong to CDR.

<sup>b</sup> CDR3 residues contacting the remaining VHH, the antigen, or both are aligned in the column on the left, right, or middle, respectively.

<sup>c</sup> Residues of the antigen having atoms within 4.0 Å to the antibody.

<sup>d</sup> Cys residues connected by a disulfide bond.

binding capacity in absence of a VL. The VH residues at positions 11, 37, 44, 45, and 47 are all conserved, hydrophobic, and are involved in interdomain contacts (1, 32, 35). In the VHHs, these residues are substituted, more hydrophilic, accessible to solvent (20), and increase the solubility of the isolated VHH domains (40, 41). The Trp-103 is another amino acid that is crucial for the interaction with a VL domain (35) and absolutely conserved in VH (98.8% occurrence) (1, 42). This Trp-103 is maintained within all the VHHs of reported structure; however, the side chain rotates ~180° about the C $\beta$ -C $\gamma$  bond to expose its most polar part, the Ne atom, to solvent (Fig. 3C). As found in ~10% of the VHHs, Arg occupies position 103 in cAb-CA05 (Fig. 1). Obviously, this W103R mutation changes the nature of the 'former VL' surface even more drastically without disturbing the main chain conformation (Fig. 3D). The hydrophobic part of the Arg side chain integrates well with the neighboring hydrophobic side chains, whereas the guanido group extends into the solvent. From the present structure we infer that the W103R mutation on a human VH might form a better choice than the framework 2 mutations (41) to render isolated VHHs more soluble. Such strategy for camelizing a VH would keep the domain more human-like. We think that a domain with the conserved human sequence at its framework 2 and carrying an Arg-103 might behave as a VHH because such sequences were found as part of heavy chain antibodies, *e.g.* clones 12 and 14 of llamas HCAs (20). In addition, it might be envisaged to humanize a camel VHH by bringing the framework 2 VHH hallmarks to the conventional human VH sequence and by substituting the Trp-103 into Arg.

From the available structural information of the antigen-binding loops of VHHs it seems that the classification of canonical structures needs to be extended (19). A new canonical structure type-4, adopted by the CDR1 loops of cAb-Lys3 and cAb-RN05, was already introduced (5, 19). In addition, the anti-human chorionic gonadotropin (hcg) and anti-hapten

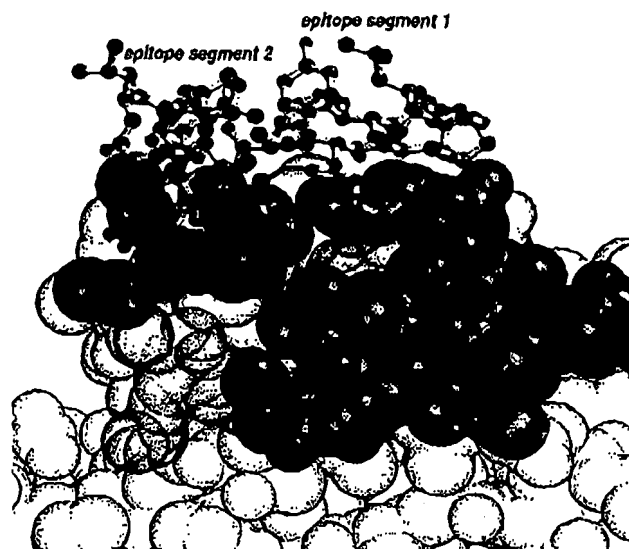


FIG. 5. The antigen-binding site of cAb-CA05. The cAb-CA05 is shown with the scaffold atoms in gray. CDR1 atoms in blue, CDR2 atoms in green. The CDR3 atoms that interact with the antigen are in red for hydrogen bonding, orange for van der Waals contacts, and black for salt bridge. The Kabat numbering of the amino acids to which the contacting atoms belong is given for reference. The carbonic anhydrase epitope segments 1 (pink dots) and 2 (red dots) are in ball-and-stick representation.

llama (RR6) VHHs exhibit a non-conventional H1 loop structure. It is shown here for the first time that the H1 loop of VHHs can be assigned to a type-1 canonical structure. This proves that the determinants of the type-1 H1 loop conformation are not *a priori* different for a VHH domain. Moreover, the Cys-33 forming an interloop disulfide bond with a Cys in the middle of the CDR3 loop is compatible with a canonical type-1 structure in cAb-CA05 and a type-4 structure in cAb-Lys3. It is therefore clear that Cys-33 is not a determinant for the H1 loop conformation.

The H2 loop of the cAb-CA05 is special because it contains only four amino acids instead of the conventional five, six or eight residues. Structurally, the H2 loop of four amino acids forms a regular  $\beta$ -turn of type II' (37). Because H2 loops of this length are absent in germline VHHs (43), they are generated by a somatic mutation.

The long CDR3 loops of cAb-CA05 are divided based on distinct functions into an N-terminal and a C-terminal part, with the Cys-100c residue as midpoint making an interloop disulfide bond. A similar loop division was introduced in the CDR3 of cAb-Lys3 (6). The C-terminal part of both CDR3-loops is involved in extensive interactions with residues that constitute the VL-interacting surface of a VH in normal VH-VL pairs. Thus, the CDR3 loop covers the remaining hydrophobic patches in this area of the domain and shields these from the aqueous solvent. With the exception of the llama hcg VHH with its short CDR3 of eight amino acids, all VHHs of known structure share this feature. The VHH-specific amino acids Phe-37, Arg-45, and Gly-47 are all contacted by the CDR3 residues (Table II), supporting the idea that it is the combined effect of these hallmark VHH substitutions and the (C-end of the) long CDR3 that provides the optimal single-domain properties of a VHH. To fulfill this role, the CDR3 of VHHs adopts a conformation that deviates fundamentally from the CDR3 of VHs. Indeed, the rules introduced to predict the CDR3 loop structures in VHs (44–46) do not apply for the CDR3 of VHHs since parts of the CDR3 are used to cover the side of the domain that interacts

with the VL in a VH-VL heterodimer. Furthermore, this novel CDR3 positioning in VHHs strongly suggests that the mutagenesis of the framework 2 amino acids of a VH to mimic the VHH of camelids will be insufficient to convert a VH into a functional, soluble single-domain antibody fragment. Additional CDR3 mutagenesis in a camelized VH will be a prerequisite to restore the antigen binding characteristics of the parental VH domain. This is exactly what the group of Riechmann (47) encountered when they used a camelized human VH to generate single-domain molecular recognition units.

The N-terminal part of the CDR3 of cAb-CA05 folds back over the CDR1 and CDR2. Both the N-terminal and the C-terminal part of the CDR3 participate in carbonic anhydrase binding (Table II). However, the residues of the N-terminal part that interact with the remaining CDR loops of the VHH domain bind with the antigen as well, whereas the C-terminal part of the CDR3-loop shows an alternating pattern of residues contacting either the antigen or the remaining VHH domain.

The N and C-terminal part of the CDR3 of cAb-CA05 forms one large surface that is essentially flat. Two marginal notes can be made from this observation. First, although this paratope architecture is also provided by the six hypervariable loops in the VH-VL heterodimers to recognize large antigens such as proteins, the difference is that the cAb-CA05 paratope is composed by CDR3 residues only. The concentration of the paratope into one single loop opens opportunities to design smaller peptidomimetics (9) or to randomize these residues and to create a synthetic library from which binders with new specificities could be retrieved by the phage display technology (48) or ribosome display (49). Secondly, it seems that the paratope of VHHs bears a large structural diversity including the formation of a flat surface as in cAb-CA05, a protruding loop as seen for the N-terminal part of the CDR3 of cAb-Lys3, or a cavity between the CDRs as observed for the hapten binder RR6. These VHHs contain a long CDR3 of 19, 24, and 16 residues, respectively. The N-terminal part of the long CDR3 of cAb-Lys3 protrudes from the remaining antigen-binding site and provides ~70% of the antigen binding surface by insertion into a cavity harboring the catalytic site of the lysozyme (6, 21). In contrast, in cAb-CA05 we are confronted with a long CDR3 that forms a planar surface that does not insert into a cavity on the antigen surface. It explains the failure of this antibody fragment to inhibit the enzymatic activity of its antigen. Furthermore, it proves that different parts of the carbonic anhydrase with a planar or a concave surface are antigenic for heavy chain antibodies carrying a long CDR3.

**Acknowledgments**—We thank M. Vanderveken for technical assistance, M. A. Ghahroudi and M. Lauwereys for initial cAb-CA05 biochemical characterizations.

## REFERENCES

- Padlan, E. A. (1994) *Mol. Immunol.* 31, 169–217
- Hamers-Casterman, C., Atarhouch, T., Muyldermans, S., Robinson, G., Hamers, C., Bijlman, S., Bendahman, N., and Hamers, R. (1993) *Nature* 363, 446–448
- Muyldermans, S., and Lauwereys, M. (1999) *J. Mol. Recognit.* 12, 1–10
- Muyldermans, S., Atarhouch, T., Saldanha, J., Barbosa, J. A. R. G., and Hamers, R. (1994) *Protein Eng.* 7, 1129–1135
- Decanniere, K., Desmyter, A., Lauwereys, M., Ghahroudi, M. A., Muyldermans, S., and Wyns, L. (1999) *Structure* 7, 361–370
- Desmyter, A., Transue, T. R., Arhbi Ghahroudi, M., Dao-Thi, M.-H., Poortmans, F., Hamers, R., Muyldermans, S., and Wyns, L. (1998) *Nat. Struct. Biol.* 5, 803–811
- Spinelli, S., Frenken, L., Bourgeois, D., de Ron, L., Bos, W., Verrips, T., Anguille, C., Cambillau, C., and Tegoni, M. (1998) *Nature Struct. Biol.* 5, 752–757
- Spinelli, S., Frenken, L., Hermans, P. W. J., Verrips, T., Brown, K., Tegoni, M., and Cambillau, C. (2000) *Biochem.* 39, 1217–1223
- Sheriff, S., and Constantine, K. L. (1996) *Nature Struct. Biol.* 3, 733–736
- van der Linden, R., de Geus, B., Stok, W., Bos, W., van Wassenaar, D., Verrips, T., and Frenken, L. (2000) *J. Immunol. Methods* 240, 185–195
- Ghahroudi, M. A., Desmyter, A., Wyns, L., Hamers, R., and Muyldermans, S. (1997) *FEBS Lett.* 414, 521–528
- Lauwereys, M., Ghahroudi, M. A., Desmyter, A., Kline, J., Hölzer, W., De Geus, B., Wyns, L., and Muyldermans, S. (1998) *EMBO J.* 17, 3512–3520
- Frenken, L., van der Linden, R. H. J., Hermans, P. W. J., Bos, W., Ruuls, R. C., de Geus, B., and Verrips, T. (2000) *J. Biotechnol.* 78, 11–21
- van der Linden, R. H. J., Frenken, L., de Geus, B., Hermans, P. W. J., Ruuls, R. C., Stok, W., de Ron, L., Wilson, S., Davis, P., and Verrips, T. (1999) *Biochim. Biophys. Acta* 1431, 37–46
- Al-Lazikani, B., Lesk, A. M., and Chothia, C. (1997) *J. Mol. Biol.* 273, 927–948
- Chothia, C., Lesk, A. M., Gherardi, E., Tomlinson, I. M., Walter, G., Marks, J. D., Llewellyn, M. B., and Winter, G. (1992) *J. Mol. Biol.* 227, 799–817
- Chothia, C., and Lesk, A. M. (1987) *J. Mol. Biol.* 186, 901–917
- Chothia, C., Lesk, A. M., Tramontano, A., Levitt, M., Smith-Gill, S. J., Air, G., Sheriff, S., Padlan, E. A., Davies, A. H., Tulip, W., Colman, P. M., Spinelli, S., Alzari, P. M., and Poljak, R. (1989) *Nature* 342, 877–883
- Decanniere, K., Muyldermans, S., and Wyns, L. (2000) *J. Mol. Biol.* 300, 83–91
- Vu, K. B., Ghahroudi, M. A., Wyns, L., and Muyldermans, S. (1997) *Mol. Immunol.* 34, 1121–1131
- Transue, T. R., De Geus, B., Ghahroudi, M. A., Wyns, L., and Muyldermans, S. (1998) *Protein: Structure, Function, and Genetics* 32, 515–522
- Ostrowski, Z. (1993) in *Proceedings of the CCP4 Study Weekend* (Swayer, L., Isaacs, N., and Bailey, S., eds.) pp. 107–113, CLRC Daresbury Laboratory, Warrington, England
- Collaborative Computational Project, Number 4. (1994) *Acta Crystallogr. D* 50, 760–763
- Navaza, J. (1994) *Acta Crystallogr. A* 50, 157–163
- Brünger, A. T. (1992) *A system for X-ray Crystallography and NMR, X-PLOR Version 3.1*. Yale University Press, New Haven, CT
- Murahudov, G. N., Vagin, A. A., and Dodson, E. J. (1997) *Acta Crystallogr. D* 53, 240–255
- Lamzin, V. S., and Wilson, K. S. (1998) *Acta Crystallogr. D* 48, 129–147
- Brünger, A. T., Adams, P. D., Clore, G. M., DeLano, W. L., Gros, P., Grasse, K., Kuszewski, R. W., Jiang, J.-S., Kuszewski, J., Nilges, M., Pannu, N. S., Read, R. J., Rice, L. M., Simonson, T., and Warren, L. (1998) *Acta Crystallogr. D* 54, 906–921
- Hubbard, S. J., and Thornton, J. M. (1993) in *NACCESS Computer Program, Version 2.1.1*, Dept. of Biochemistry and Molecular Biology, University College London, UK
- Kraulis, P. J. (1991) *J. Appl. Crystallogr.* 24, 946–950
- Merritt, E. A., and Murphy, M. E. (1994) *Acta Crystallogr. D* 50, 869–873
- Kabat, E. A., Wu, T. T., Perry, H. M., Gottesman, K. S., and Foeller, C. (1991) *Sequence of Proteins of Immunological Interest*, Publication 91-3242 U.S. Public Health Services, National Institutes of Health, Bethesda, MD
- Chothia, C., Gelfand, I. M., and Kister, A. E. (1998) *J. Mol. Biol.* 278, 487–479
- Chothia, C., Boswell, D. R., and Lesk, A. M. (1988) *EMBO J.* 7, 3745–3755
- Chothia, C., Novotny, J., Brucoleri, R., and Karplus, M. (1985) *J. Mol. Biol.* 188, 651–663
- Riechmann, L. (1996) *J. Mol. Biol.* 259, 957–969
- Hutchinson, E. G., and Thornton, J. M. (1996) *Protein Sci.* 5, 212–220
- Hermans, M. M., Ruuls, R. C., Nijman, I. J., Niewold, T. A., Frenken, L., and de Geus, B. (2001) *Mol. Immunol.* 37, 579–590
- Padlan, E. A. (1996) *Adv. Protein Chem.* 49, 67–133
- Davies, J., and Riechmann, L. (1996) *Proc. Eng.* 9, 531–537
- Riechmann, L., and Muyldermans, S. (1993) *J. Immunol. Meth.* 231, 25–38
- Kabat, E. A., and Wu, T. T. (1991) *J. Immunol.* 147, 1709–1719
- Nguyen, V. K., Hamers, R., Wyns, L., and Muyldermans, S. (2000) *EMBO J.* 19, 921–931
- Shirai, H., Kidera, A., and Nakamura, H. (1999) *FEBS Lett.* 455, 188–197
- Shirai, H., Kidera, A., and Nakamura, H. (1995) *FEBS Lett.* 369, 1–8
- Morea, V., Tramontano, A., Rustici, M., Chothia, C., and Lesk, A. M. (1998) *J. Mol. Biol.* 275, 269–294
- Davies, J., and Riechmann, L. (1995) *Biotechnology* 13, 475–479
- Hoogenboom, H. R., de Bruine, A. P., Hufon, S. E., Hoet, R. M. A., Arends, J. W., and Roovers, R. C. (1998) *Immunotechnology* 4, 1–20
- Schaffitzel, C., Hones, J., Jermutus, L., and Plückthun, A. (1999) *J. Immunol. Methods* 231, 119–136
- Fan, Z. C., Shan, I., Guddat, L. W., He, X. M., Gray, W. R., Raison, R. L., and Edmundson, A. B. (1992) *J. Mol. Biol.* 228, 188–207

Nature. 1986 May 29-Jun 4;321(6069):522-5.

Replacing the complementarity-determining regions in a human antibody with those from a mouse.  
Jones PT, Dear PH, Foote J, Neuberger MS, Winter G.

The variable domains of an antibody consist of a beta-sheet framework with hypervariable regions (or complementarity-determining regions--CDRs) which fashion the antigen-binding site. Here we attempted to determine whether the antigen-binding site could be transplanted from one framework to another by grafting the CDRs. We substituted the CDRs from the heavy-chain variable region of mouse antibody B1-8, which binds the hapten NP-cap (4-hydroxy-3-nitrophenacetyl caproic acid; KNP-cap = 1.2 microM), for the corresponding CDRs of a human myeloma protein. We report that in combination with the B1-8 mouse light chain, the new antibody has acquired the hapten affinity of the B1-8 antibody (KNP-cap = 1.9 microM). Such 'CDR replacement' may offer a means of constructing human monoclonal antibodies from the corresponding mouse monoclonal antibodies.